CHAPTER 3

The Measurement of Natural Hydrogen Sulfide and Sulfur Dioxide Emission from Agricultural Soil and Volcanic Gases at Mt. Aso

3.1. Abstract

Agricultural soils are thought to important sources of sulfur gases to the atmosphere. Emission of sulfur dioxide and hydrogen sulfide gases from model agricultural was investigated. Emission was investigated from model agricultural field with and without fertilizer. Emission variability also observed with respect to soil physical conditions. Mean emission rate as SO_2 and H_2S from the four different model fields were 23.98±14.17 and 2.07±3.46 (without fertilizer), 29.39±14.25 and 2.09±4.14 (natural fertilizer), 7.81±5.05 and 2.09±3.98 (chemical fertilizer), 9.02±7.83 and 2.63±4.57 $\mu gS\ m^{-2}\ h^{-1}$ (mixed fertilizer) obtained. Very fluctuation of SO_2 emission was observed compare to the emission of H_2S. SO_2 emission was significantly influenced by the soil physical properties e.g. soil moisture content and soil surface temperature. Significant emission was observed from this kind of agricultural field, although, the mechanism of emission is not clear.

3.2. Introduction

Interest and research in volatile sulfur compounds have developed rapidly during the last decade because of their reported contribution to air pollution, climatic effects and precipitation chemistry.[1-3] In biogeochemistry, the sulfur cycle is one of the most complex cycles because oxidation of sulfur varies between - 2 and + 6 and there are a large variety of organic and inorganic species. Large uncertainties remain concerning the chemical species and the magnitude of natural emission of sulfur gases into the atmosphere. Several authors reported about sulfur emission from natural sources e.g. wet land, marine tidal flat, soil and vegetation, rice field, sea water etc. However, the reported rates of sulfur gas emission span several orders of magnitude, which creates a large uncertainty in the global atmospheric sulfur budget.[4,5]

Currently recognized sources for atmospheric sulfur dioxide are volcanism, biomass burning, smelting of sulfidic ores, burning of fossil fuels, and atmospheric oxidation of biogenic, volatile organic sulfur compounds, emitted from oceans, soils and vegetation. Soils have long been recognized as SO_2 sinks, However, the possibility of SO_2 emission from

these soils has been questioned because they are generally moist and SO_2 is extremely soluble.[7] Macdonald *et al.*,[8] reported that acid sulfate soil can emit SO_2 directly to the atmosphere. In our previous study (Chapter 2), we observed that marine tidal sediment can emit SO_2 to the atmosphere even the neutral kind of sediment. There are a few work has been done on the emission of SO_2 from the soil. All over the world it has huge amount of cultivated land. Sulfur gases are generated in the sediment through complex chemical and bio-chemical processes during the decomposition of organic matter and sulfate reduction.[9,10] The aim of this work was to investigate the emission of SO_2 and H_2S from the agricultural soil and their influencing factor e.g. soil water content, fertilizer soil surface temperature and also from active volcano Mt. Aso.

3.3. Materials and Methods

3.3.1. Preparation of Agriculture Field and Measurement of Soil Properties

Five different garden were prepared depend of fertilizer addition for the investigation of effect of fertilizer on emission. The agriculture fields were prepared in the Kumamoto University garden on May 12, 2005 and after one week the emission measurement were started. The garden was watered two/three times in a week. The paddy field was watered every day at the first two weeks such that the garden was flood with 3-5 cm depth water level. From third week the rice field was watered as same way but twice/thrice in a week. The soil moisture content was continuously observed by using a pF meter. pF a unit formerly used in agricultural science to measure "soil suction" or soil moisture tension. Soil moisture tension is the pressure that must be applied to the moisture in the soil to bring it to hydraulic equilibrium with an external pool of water. This was measured in pF units as the logarithm of the pressure in centimeters of water. Temperatures of the soil surface, sample air and the instrument inside were monitored simultaneously with platinum temperature sensors.

Table 3.1.
Types of agriculture garden for emission measurement

Name	Area	Kind of fertilized added	Plant of vegetation
Garden 1 (G1)	1 m x 1m	No fertilizer added	Egg plant and patchy grass
Garden 2 (G2)	1 m x 1m	Natural (7 kg)	Egg plant and patchy grass
Garden 3 (G3)	1 m x 1m	Ammonium Sulfate (1 kg)	Egg plant and patchy grass
Garden 4 (G4)	1 m x 1m	Ammonium Sulfate (1 kg) and Natural (7kg)	Egg plant and patchy grass
Garden 5 (G5)	1 m x 1m	No fertilizer added	Paddy field

3.3.2. Dynamic Chamber Sampling System for Soil Emission and Instrument for On-Site Measurement

The instrument described in the section 2.3.3 was used for on-site measurement of gases. The instrument was calibrated with standard gas before and after the measurement campaign. A chamber made of polypropylene 21 cm w x 28 cm d x 9.5 cm h (sampling surface area 0.0588 m^2, volume of the chamber 5.8 l), and had two ports for air inlet and outlet was used for emission measurement. The system carried to the garden and emission was measured in daytime. A Nafion dryer was attached to the sampling chamber outlet to remove the moisture from the sample air. The chamber was placed on the soil surface and continuously measured the emission for 10 min, before and after the surface measurement the ambient concentration was measured. During the atmospheric gas measurement, the chamber was removed from the soil surface to avoid heat condensed in the chamber. The emitted gas concentration was calculated by subtracting the ambient concentration from the chamber gas concentration. Sulfur emission rate was calculated according to the equation 3.1 using the chamber gas level and chamber surface area. Mobile campaigns were conducted for measurement of SO_2 and H_2S concentration in the volcanic gases at Mt. Aso. The gases was measured by walk around the crater and mounted the instrument on the bank of the crater lake. When computer was used for operate the instrument Gas Analyzer software was used for controlling the calibration and measurement mode, data acquisition and data processing. Figure 3.2 shows the flow chart of operation and window of Gas Analyzer software in the computer screen.

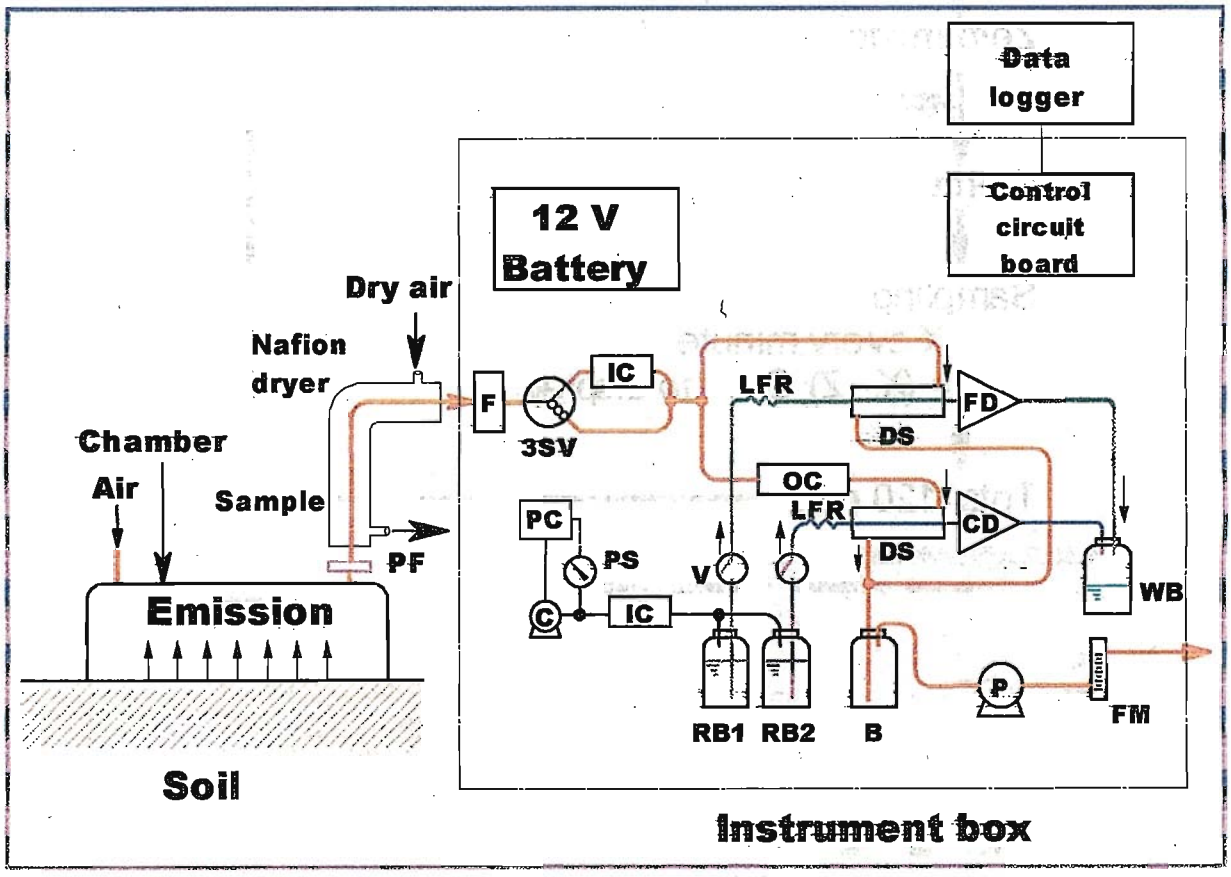

Figure 3.1. Sampling/measurement system for simultaneous measurements of H_2S and SO_2 emissions at soil. HP: heating pads, F: inlet filter, 3SV: three-way solenoid valve, IC: iodinated activated charcoal/sodalime column, OC: oxalic acid column, FM: flow meter, B: flow buffer bottle, P: air pump, PC: pressure control circuit, PS: pressure sensor, C: miniature compressor, RB1: FMA reagent bottle, RB2: H_2SO_4/H_2O_2 reagent bottle, V: stop valve, LFR: liquid flow restrictor, FD: fluorescence detector, CD conductivity detector, WB: waste bottle, DS: diffusion scrubber with porous polypropylene tube, PF: paper filter.

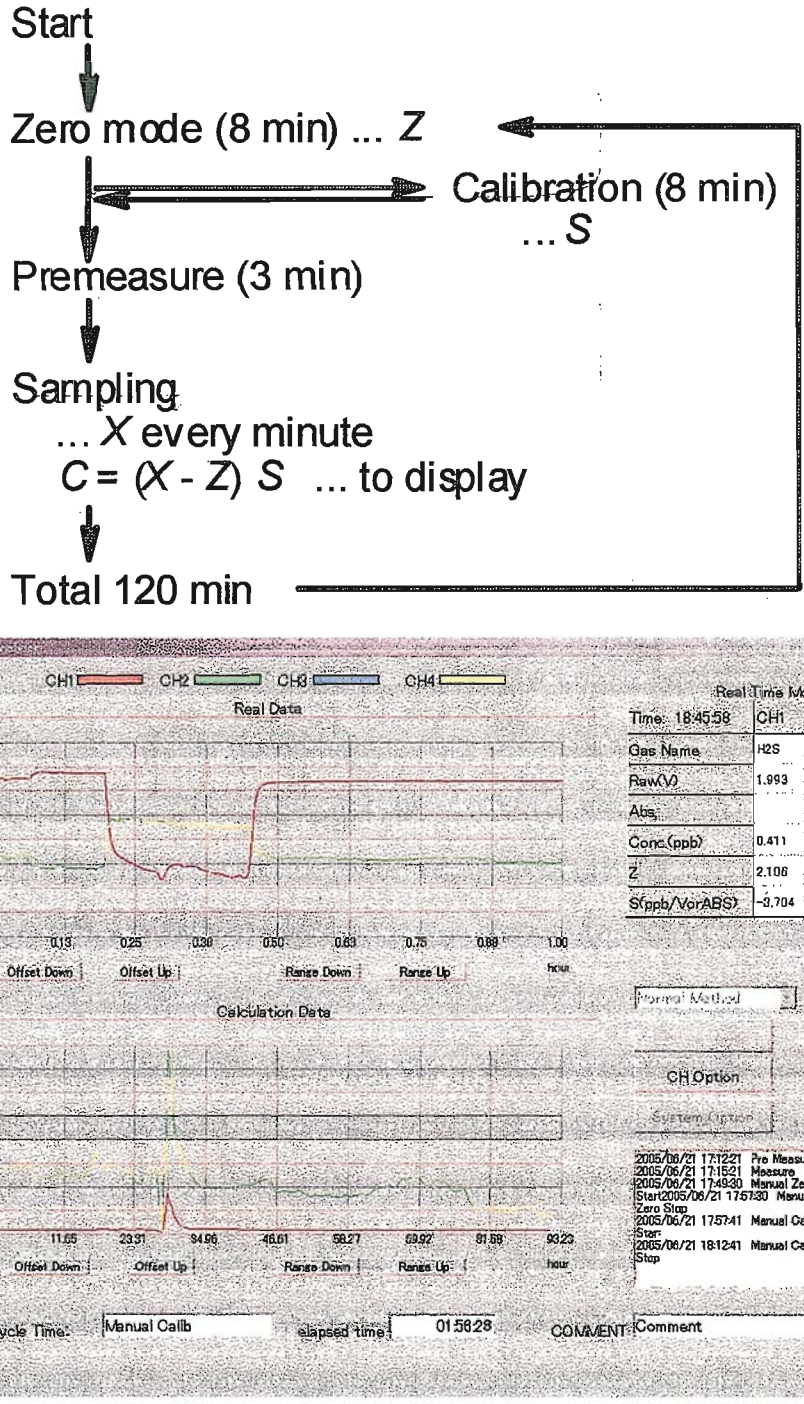

Figure 3.2. Program for system control, data acquisition and data processing. Flow chart of the operation procedure (above) and display in the computer screen (below).

The carbon dioxide concentration was also monitored simultaneously by a CO_2 monitor (Model RI-215A (Type-2000-A), Riken Keiki, Japan) in the sample air, since CO_2 interfere the SO_2 measurement. Agricultural soils emit significant amount of CO_2 to the atmosphere.

In our measurement soil emitted CO_2 level was 50 to several hundreds ppmv. To investigate CO_2 interference 50-1000 ppm standard CO_2 gas was tested by the instrument used for soil emission measurement. Negligible interference was observed if CO_2 level below 200 ppm. During the calculation of SO_2, the corresponding CO_2 response was subtracted from the instrument response for SO_2. Ammonia also interfere the measurement of SO_2. Since soil emit ammonia, to avoid interference from ammonia oxalic acid column (OC) was used in front of the SO_2 collecting sampling line. Interference from nitrogen dioxide was also investigated. Figure 3.3 shows that interference from NO_2 was negligible. The measurement was performed during May to September 2005.

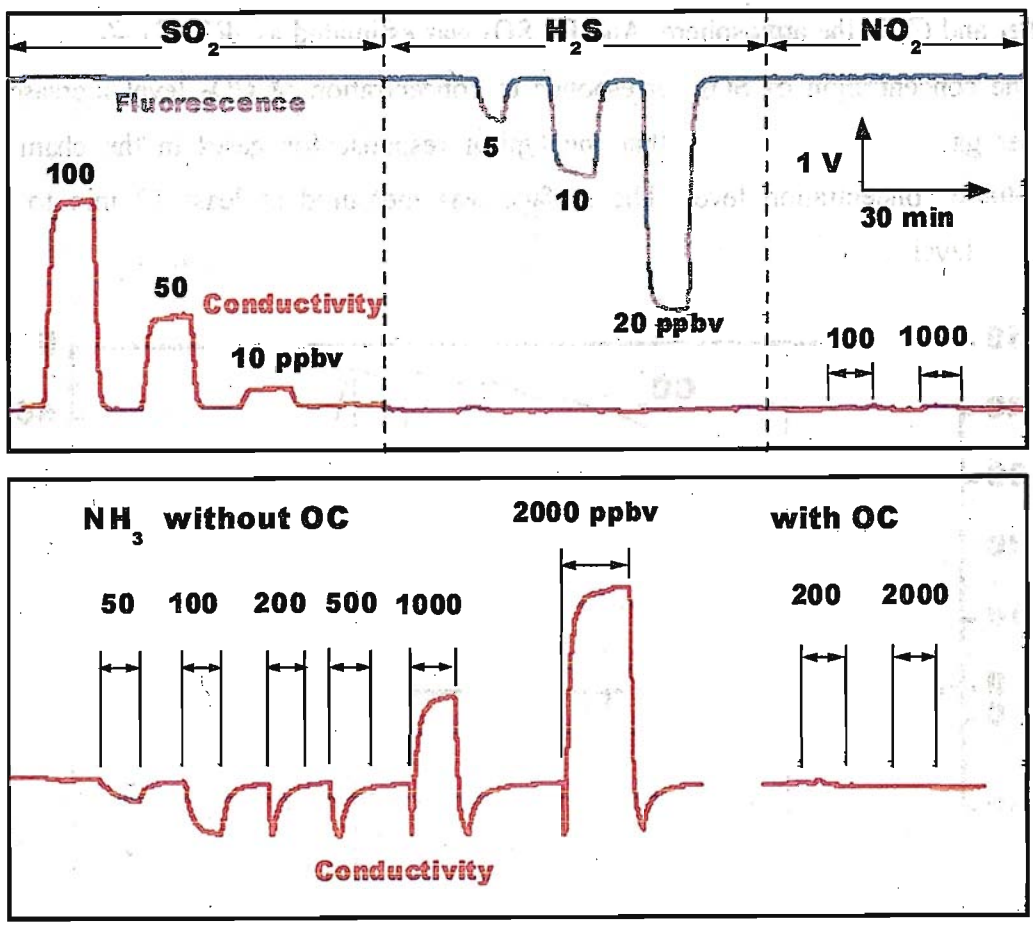

Figure 3.3. Response of fluorescence and conductivity signals to SO_2 and H_2S. NO_2 did not interfere and NH_3 interference was eliminated by oxalic acid (OC) column. Flow rates of the absorbing solutions and sample air were 160 ml min^{-1} and 0.70 l min^{-1}, respectively.

3.4. Results and Discussion

3.4.1. Measurement of Gas Emission from Soil

The atmospheric level of gas concentration was measured before and after the chamber gas measurement. The chamber gas level was increased due to emission from soil. Emission rates, E, in μgS m^{-2} h^{-1} were determined from these increases in the gas concentrations (ΔC, ppbv) in the sample air confined by the chamber with the area of "A" m^2 and the total air sampling rate (F, l min^{-1} as the standardized flow at 0 °C and 1 atm):

$$E = 32.1 \times 10^6 (\Delta C \times 10^{-9}) (60\,F) / 22.4\,A \quad \ldots\ldots (3.1)$$

ΔC for H_2S was estimates as $\Delta C = C_H - C_A$, where C_H is the concentration of gases in the chamber and C_A in the atmosphere. And for SO_2 was estimated as $\Delta C = C_H - (C_A + C_i)$, where C_i is the concentration of SO_2 corresponds to concentration of CO_2 level increase in the chamber gas. Figure 3.4 shows that the typical response for gases in the chamber and atmospheric concentration level. The surface was measured at least 10 min to get the saturation level.

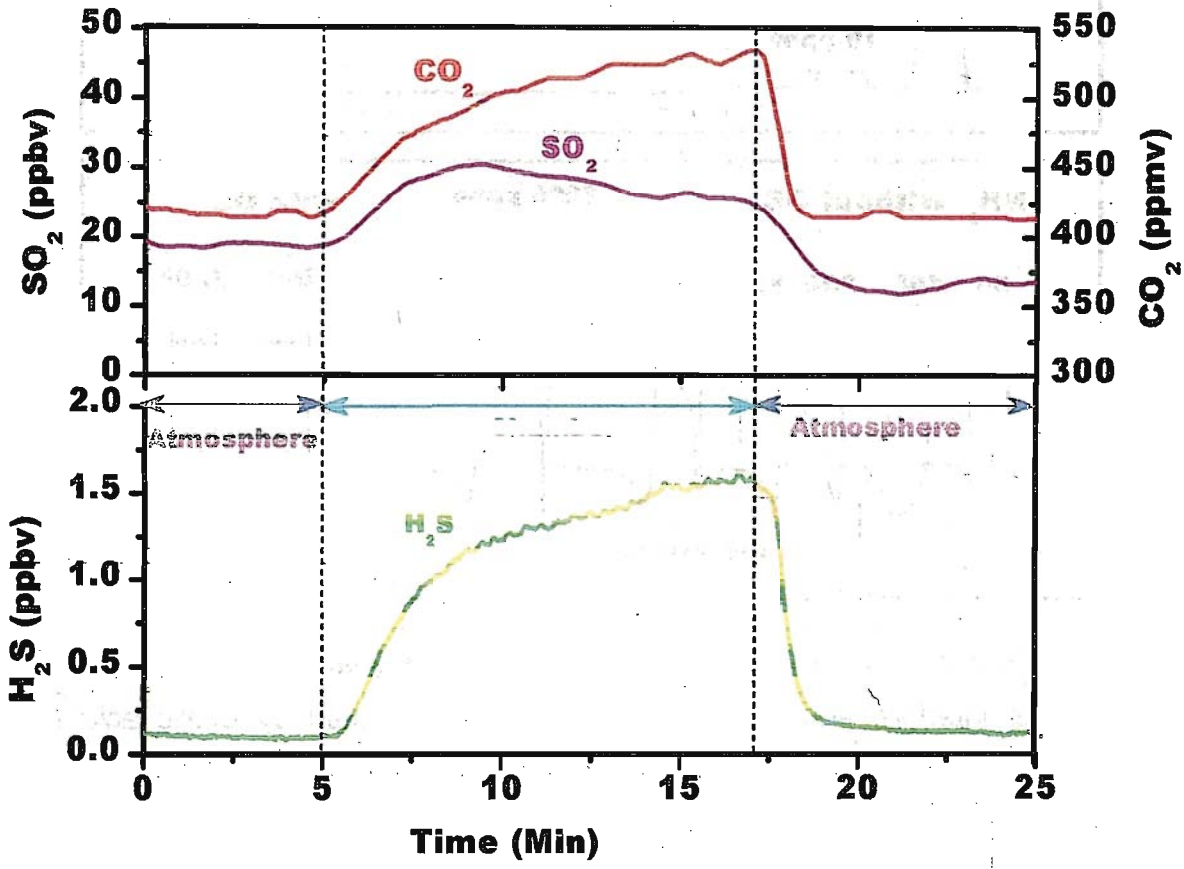

Figure 3.4. Typical response for gases H_2S, SO_2 and CO_2 level in the atmospheric and sampling chamber. The chamber gas was measured at least 10 min to get the saturation point.

3.4.2. Effect of Fertilizer on Emission of Gases

There was a negligible trend of emission observed with time during the measurement period (May to September, 2005). The estimated emission rate of sulfur as H_2S and SO_2 in five different gardens of No fertilizer, with natural fertilizer, chemical fertilizer, mixed fertilizer and paddy field without fertilizer are shown in Figure 3.5 G1, G2, G3, G4, G5. Table 3.2 shows that, the average emission rate of sulfur, as SO_2 during the measurement period, was observed highest at the garden 2 (natural fertilizer content) 29.39±14.25 μgS m^{-2} h^{-1} and lowest at the garden 3 (chemical fertilizer content) 7.81±5.05 μgS m^{-2} h^{-1}. Mean emission as SO_2 at garden 1, which contents no fertilizer, was higher than that of both garden 3 and garden 4 that content chemical and mixed fertilizer respectively.

Table 3.2.
Mean sulfur flux in each garden as H_2S and SO_2 during the measuring period.

Garden type	Emission rate (μgS m^{-2} h^{-1})		Fertilizer added	
	H_2S	SO_2		
Garden 1	2.07 ± 3.46	23.98 ± 14.17	No	
Garden 2	2.09 ± 4.14	29.39 ± 14.25	Natural	
Garden 3	2.09 ± 3.98	7.81 ± 5.05	Chemical	
Garden 4	2.63 ± 4.57	9.02 ± 7.83	Mixed Chemical)	(Natural,
Garden 5	1.51**	nd*	No	

*Not detected **Measurement was performed two times

Although both the organic matter and chemical fertilizer are the sources of sulfur to the soil, the reason of higher emission rate in the garden 1 and 2 was not clear here. The low emission rate in the chemical fertilizer content garden 3 and 4 compare to non chemical fertilizer content garden 1 and 2 might be due to the content of ammonium ion and which might trapped SO_2. According to the reported mechanism, acidic condition is required at the interface to emit SO_2 by the soil. In the paddy field low emission of H_2S was observed compare to the other field (Table 3.2) and SO_2 emission was not detected. During the paddy field preparation the surface soil was removed to create about 10 cm depth low land and no fertilizer was added. It is infer that the paddy had deficiency of sulfur containing organic compounds. Low biodegradable organic matter content in the paddy field might be the reason of low emission.

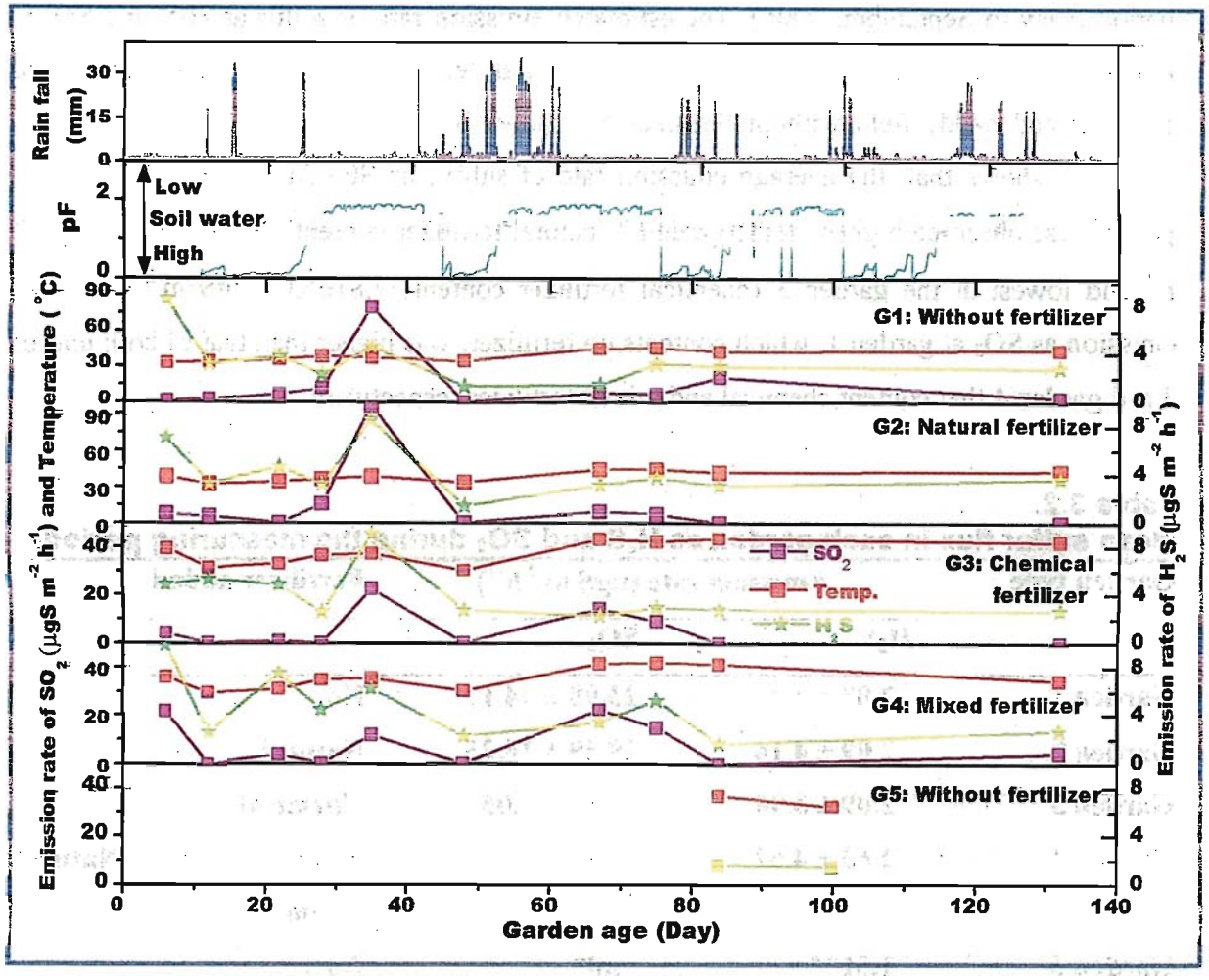

Figure 3.5. Emission of H_2S and SO_2 with garden age, soil moisture tension (pF), rain fall (The rain fall data was obtained from online source of Japan Metrological Agency, www.data.kishou.go.jp/etrn/index) and soil surface temperature. Measurement was performed in May to September, 2005. Day "0" is the garden preparation day.

3.4.3. Effect of Soil Moisture Content and Atmospheric Weather Condition on Emission

The fluxes of sulfur were investigated with respect to soil physical properties. According to the definition of pF, there is an opposite correlation between soil pF value and soil water content. Figure 3.5 shows that, the lowest pF value was observed during the rainy period when the soil was saturated with water. There were some sudden fluctuations of pF value

observed in the dry period (Figure 3.5) that was due to watering the garden. During the measurement campaigns the weather was sunny and the soil surface was dry except in June 30, 2005 measurement campaign (at day 48 of the garden age), in that day the weather was cloudy and the soil surface was moist. In the day 48 of the garden age there was no SO_2 emission observed at all of the four gardens. Figure 3.5 shows that significant emission variability was observed with soil surface temperature and soil water content in all the four gardens. Particularly, the drastic emission variability of SO_2 was observed with respect to soil surface temperature and soil water content. Highest emission rate of SO_2 was observed in the day 35 of the garden age in all the four gardens, when the temperature of the soil surface was increased and the soil contents least amount of water. Bates *et al.*[11] reported that soil physical properties (e.g. soil surface temperature) are more significant for biogenic sulfur emission than the bacterial activities. In the present investigation, also observed that both SO_2 and H_2S emission was varied with physical properties of the soil. The emissions of biogenic sulfur gases from soil are closely correlated with temperature.[12] In our experiments; the emission of sulfur gases at higher temperature was higher than at lower temperature (Figure 3.5). Figure 3.5 shows that the fluctuation of SO_2 emission was very high compare to the emission of H_2S. High reactivity and solubility in water of SO_2 than that of H_2S might be the reason of high emission fluctuation. There are various mechanisms proposed depending on the sediment and soil characteristics for the generation and emission of sulfur gases. In our pervious study we estimate mechanism for generation and emission of H_2S and SO_2 from marine sediment (Figure 2.8, Chapter 2).

3.4.4. Global Implications to Sulfur Emission

Table 3.2 shows that the mean sulfur emission as H_2S and SO_2 from the reported model agricultural soil with the area of $1m^2$. According to the Food and Agricultural Organization (FAO) online database source (www.faostat.org/faostat/collections) about 4.97×10^{13} m^2 total agricultural lands used in the world in 2003. Although there are a large uncertainties in the emission rate but, it could be infer that huge amount of sulfur emitted to the atmosphere from the anthropogenic influenced natural source. In the global sulfur cycle proper estimation of sulfur input to the atmosphere from these sources are required.

3.4.5. Measurement of SO_2 and H_2S at Mt. Aso

Continuous monitoring and mobile monitoring were conducted at Mt. Aso. In Oct. 2003 the measurement was conducted by walk around the crater (Figure 3.6a). In Feb. 2004 the

measurement was conducted by mounted the instrument on the edge of the cratere (Figure 3.6b). Concentration of gases in the measurement of Oct. 2004 was much higher than that of Oct. 2003 due to the higher volcanic activity.

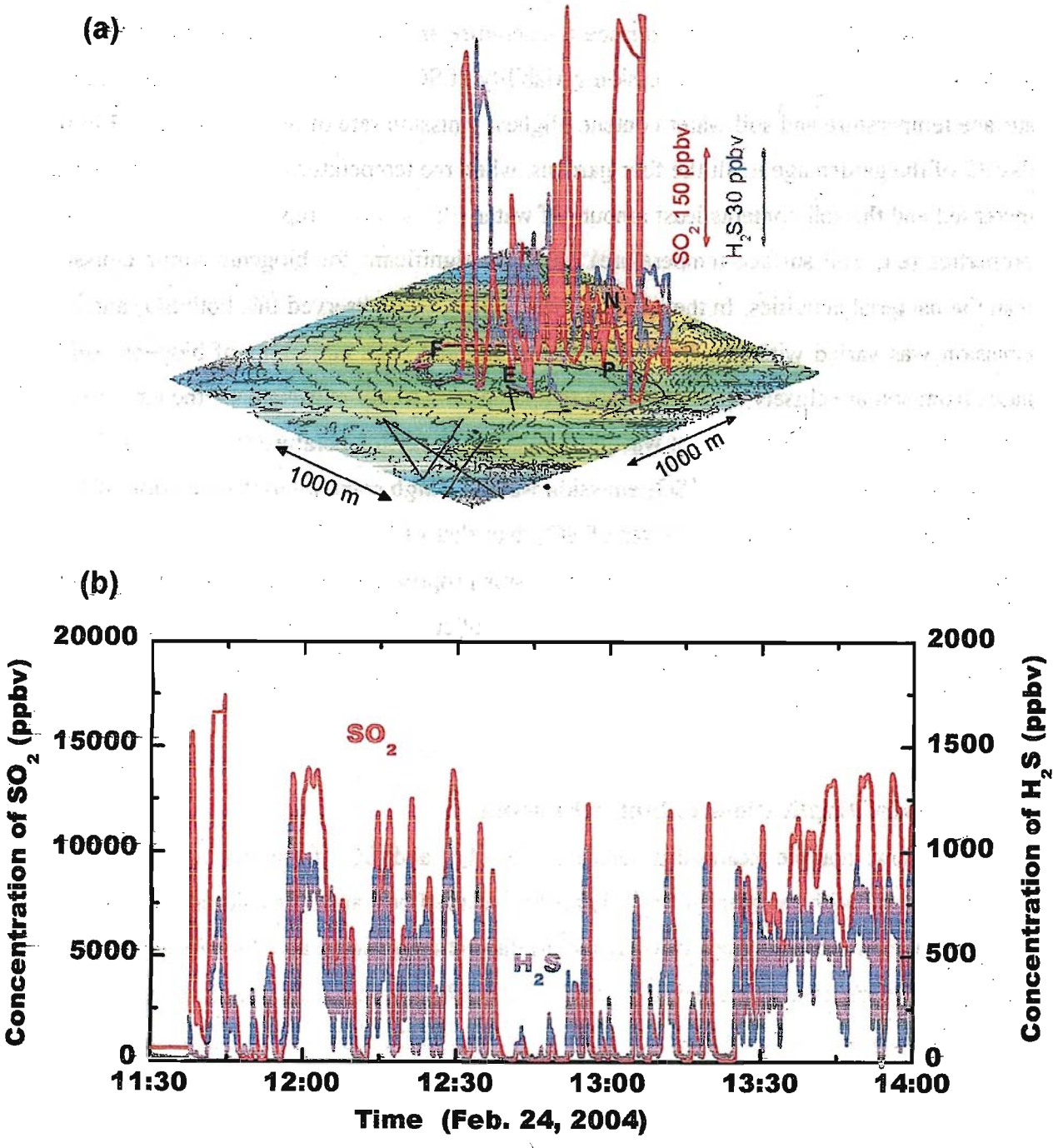

Figure 3.6. Mobile campaign data obtained around Mt. Aso crater. In (a) the gas levels are plotted on the map of Mt. Aso crater. Black lines indicate the rout we walk around with the instrument, and red and blue lines are SO_2 and H_2S gas levels. Data (b) was obtained by mounted the instrument on the crater edge without moving.

3.5. Conclusions

The result obtained through this investigation about sulfur emission from the model agricultural field was not so low compare to the emission of some marine sediment. Although the fluctuation of SO_2 emission was very high but in dry condition emission was significant. Both gases were emitted even from the garden without fertilizer. The low emission rate of SO_2 from the garden with chemical fertilizer was not clear. Due to the wide range of oxidation states of sulfur and the variety of sulfur compounds with carbon and oxygen we are a long way from understanding sulfur chemistry in natural systems

References

1. Jorgensen, B. B. and Okholm-Hansen, B., Emissions of biogenic sulfur gases from a Danish estuary. Atmospheric Environment. *Atmospheric Environment,* **19**, pp.1737–1749 (1985).
2. Staubes, R., Georgii H.-W., Ockelmann, O., Flux of COS, DMS and CS_2 from various soils in Germany. *Tellus* **41B**, pp.305–313 (1989).
3. Howarth, R.W. and Stewart J. W. B. (1992) In *Sulfur Cycling on the Continents: Wetlands, Terrestrial Ecosystems and Associated Water Bodies.* (Edited by Howarth, R. W., Stewart, J. W. B. and Ivanov, M. V.) pp. 67–84. John Wiley, Chichester.
4. Carroll, M. A., Heidt L. E., Cicerone, R. J., Prinn, R. G., OCS, H2S and CS2 fluxes from a salt water marsh. *Journal of Atmospheric Chemistry,* **4**, pp.375– 395 (1986).
5. Andreae, M.O. and Jaeschke, W.A., (1992). In *Sulphur Cycling on the Continents: Wetlands, Terrestrial Ecosystems and Associated Water Bodies.* (Edited by Howarth R.W. Stewart, J. W. B. and Ivanov, M. V.), pp. 27–61. John Wiley, Chichester.
6. Taylor, C.H., Kesler, S.E., Cloke, P.L., Sulfur gases produced by the decomposition of sulfide minerals: application to geochemil exploration. *Journal Geochemical Exploration,* **17**, pp.165–185 (1982).
7. Macdonald, B.C.T., Denmead, O.T., White, I., Melville, M.D., Natural sulfur dioxide emissions from sulfuric soils. *Atmospheric Environment,* **38**, pp.1473–1480 (2004).
8. Devai, I., DeLaune, R.D. Formation of volatile sulfur compounds in salt marsh sediment as influenced by soil redox condition. *Organic Geochemistry,* **23(4)**, pp.283-287 (1995).
9. Canfield, D.E., Thamdrup, B. Fate of elemental sulfur in an intertidal sediment. *FEMS Microbiology Ecology,* **9,** pp.95-103 (1996).
10. Bates, T.S., Lamb, B.K., Guenter, A., Dignon, J., Stoiber, R.E., Sulfur emission to the atmosphere from natural sources. *Journal of Atmospheric Chemistry,* **14**, pp.315–337 (1992)
11. Goldan. P. D., Kuster, W. C., Albritton D. L., Fehsenfeld, F. C., The measurement of Natural sulfur emissions from soils and vegetation: Three sites in the eastern United States revised. *Journal of Atmospheric Chemistry,* **5,** pp. 439-467(1987).

CHAPTER 4

On-site Measurement of Methyl Mercaptan and Dimethyl Sulfide by Single Column Trapping/Separation and Chemiluminescence Detection

4.1. Abstract

Simple and automated method for measurement of methyl mercatan and dimethylsulfide has been investigated. These two are the most odorous among the sulfur gases. The collection and subsequently separation are performed with a single short column packed with silica gel adsorbent without any additional separation column. CH_3SH and DMS are separated according to their desorption temperatures and introduced into a chemiluminescence cell in the same order. These two gases are detected based on the strong chemiluminescence reaction with ozone. Linearity of calibration curves with this system is advantageous compared to flame photometric detector. The total system, including a small cylinder for the carrier nitrogen, can be set in a carriable box. The instrument is applicable to breath odor analysis. Also, automated and continuous measurement of room air could be performed with this instrument. During continuous three days toilet air analysis, it was observed that the sulfur gases level increased after becoming dark. The sulfur gases in ppbv level are successfully measured without any big interference and complicated experimental procedure.

4.2. Introduction

Presence of volatile sulfur compounds (VSCs) in waste gases deserves special attention due to their very low odor threshold value (for methyl mercaptan 0.4 ppb), high toxicity and potential corrosive effect.[1-5] The monitoring of VSCs is important for natural environment researches and clinical diagnoses as well. VSCs are emitted from sediments especially in coastal area[6] and converted into SO_2 and sulfate to contribute to the climate as the cloud condensation nuclei. Dimethylsulfide (DMS) is one of the characteristic gases emitted from seawater surface and alga. Also, VSCs are known to be key contributors to halitosis.[7-13] The intensity of clinical bad breath is significantly correlated with the level of the intraoral VSCs.[14,15] Methylmercaptan, CH_3SH, shows independent association with noticeable oral malodor and more useful marker than H_2S.[16] Odors of CH_3SH and DMS are heavier than that of H_2S. Breath analysis has attracted a considerable amount of scientific and clinical interest during the last decade. Exhaled levels of sulfur containing compounds are elevated in liver failure and allograft rejection.[17] Looking at a set of volatile markers may enable recognition

and diagnosis of complex diseases such as lung cancer. Due to technical problems of sampling and analysis and a lack of normalization and standardization, huge variations exist between results of different studies. This is among the main reasons why VSC breath analysis could not yet been introduced into clinical practice.[17]

It is generally difficult to collect, storage and analyze VSCs at trace levels because of their highly adsorptive, reactive and volatile properties. The VSC analyses require preconcentration because most substance concentration in environmental and breath sample fall in ppbv–pptv ranges. Adsorption on solid adsorbents, such as Tenax and β,β'-ODPN, and subsequently measured by gas chromatography with sulfur selective detector e.g. flame photometric detector, GC-FPD,[4,18,19] GC-PFP[20] is common practice for VSC determinations. GC-MS is also popular recently for VSC analysis[21] sometimes combined with three-stage cryogenic trapping system to reduce suffering from huge amount of CO_2 present in the breath air.[22] Solid phase microextraction (SPME) is also one of the strategies to sample the volatile sulfur gases.[23-25]

The light emitting species is generated not only by the reducing flame in FPD but also by the reaction with ozone. Consequently, VSCs can be detected by chemiluminescence measurement. The chemiluminescence spectrum extends from 280–400 nm and is centered around 360 nm.[26-28] Kelly *et al.*[29] combined a commercial NO chemiluminescence instrument with GC to obtain chemiluminescence chromatogram for VSCs. Sulfur chemiluminescence detector (SCD), based on conversion into SO in a furnace and ozone induced chemiluminescence, have become one of the most powerful tools to analytical chemist.[30,31] The first step needs high power and high temperature conversion with H_2[32] to obtain nearly equal sensitivity on a per mol of sulfur basis.[33] However, even without any pretreatment, CH_3SH and DMS directly give significant chemiluminescence signal by reaction with ozone.

The possible mechanism of chemiluminescence reaction with ozone is complicated and multi step. The first step of the reaction is not identified but, electronically excited SO_2 is identified as a light emitting species and that is generated by the reaction of SO with ozone. According to the earlier investigation, SO may be generated by the reaction with sulfur gases through a complex reaction .The final steps in the mechanism of ozone/sulfide chemiluminescence are

$$\text{Sulfur gas} + O_3 \rightarrow SO + \text{Products} \quad \text{.....(4.1)}$$

$$SO + O_3 \rightarrow SO_2^* + O_2 \quad \text{.....(4.2)}$$

$$SO_2^* \rightarrow SO_2 + h\nu \quad \text{.....(4.3)}$$

On-site measurement is ideal for VSCs analysis due to their lack in stability. No instrument is currently available for automatic measurement of VSCs to the best of our knowledge.[34] We have already developed a diffusion scrubber based instrument for continuous H_2S measurement [35,36] and applied it to volcanic gas measurements[37] and gas emission analysis at tidal flat sediments.[38] CH_3SH and DMS are more important odorous species than H_2S as mentioned above. That system has been modified to measure CH_3SH by using two kinds of membrane scrubbers.[39] However, that is indirect CH_3SH measurement, and the sensitivity and reliability were not satisfactory for CH_3SH. Here, a new method is presented for determination of the major odorous sulfur compounds, CH_3SH and DMS. This is based on a simple trap/separation system and gas-phase chemiluminescence measurement. Preconcentration and separation of gases is performed with the same column. The instrument is compact and fieldable. The present method allows on-site analysis of CH_3SH and DMS at ppb levels and is applicable to odor measurement and breath analysis.

4.3. Experimental

4.3.1. Trapping/Separation Column

A single column was used for both trapping and separation of sample gases. MTO-Davidson silica gel (grade 12, 60/80 mesh, Supelco, Bellefonte, PA) was packed in a mullite ceramic tube (2 mm id x 3 mm od x 20 cm, NewMullite®, Nikkato Co., Osaka, Japan) with silanized quartz wool plugs in the ends. The effective adsorbent bed was 14 cm long. A nickel-chrome wire (ϕ 0.2 mm x 35 cm, 15 Ω) was coiled around the ceramic tube as a heater. The heater was covered with glass wool and aluminum tape together with a thermocouple. The column temperature was regulated by a programmable temperature controller (E5AK-TAA2FB, Omron Co., Kyoto, Japan) with applying 30 V AC to the heater via a solid-state relay. Before the first use, the column was cleaned for 2 h at 330 °C with constant flow of nitrogen at 20 mL/min.

4.3.2. Chemiluminescence Detector

Figure 4.1 presents a schematic illustration of chemiluminescence cell and photomultiplier tube (PMT) arrangement. The reaction cell was constructed without any special machined part. The cell consisted of quick-coupling flange tube (25 mm id x 40 or 20 mm L, KF 25, ULVAC, Chigasaki, Japan) made of stainless steel. The inside of the tube was polished before use. Sample and ozone gases were introduced through concentric stainless steel tubes, which outer diameters were 1/8" and 1/4", respectively. An optical convex lens

(S51-20-30, Suruga Seiki, Shizuoka, Japan) and a spherical glass plate (ϕ 21 mm x t 2.5 mm) were placed at the window of the reaction cell and fixed with o-rings. The transmission of the glass plate was tested since the ozone/sulfide chemiluminescence emitted in the UV region. Figure 4.2 shows the emission spectra of DMS, % transmission of glass plate, and the photomultiplier tube (PMT).

Light generated in the reaction cell was detected by using a PMT (R3550A, Hamamatsu Photonics, Hamamatsu, Japan) placed at the window of the reaction cell. High voltage (HV) was applied to the PMT from a miniature HV supplier (OPTON-1NC-12, Matsusada Precision, Kusatsu, Japan), which was powered by 12 V DC. The PMT voltage was adjusted to be 830 V to optimize the signal-to-noise ratio. The PMT current was converted into voltage with amplification factors of 0.1 V/nA (with 100 MΩ). The signal was amplified in the main circuit board 10 times and 100 times for wide range and high sensitivity determinations, respectively.

Sensitivity of the detection system was investigated by directly introducing the standard gases to the reaction cell. The reduced sulfur gases which are most abundant in the natural atmosphere and pollution sources were tested. Ozone induced sulfur chemiluminescence detection system has potential interference from nitric oxide and some alkenes. Nitric oxide and isoprene most common in the human breath were tested as interference. Table 4.1 represents the response of the detector for most common VSCs and other gases. Methyl mercaptan and dimethyl sulfide was highly sensitive compare to the other gasess.

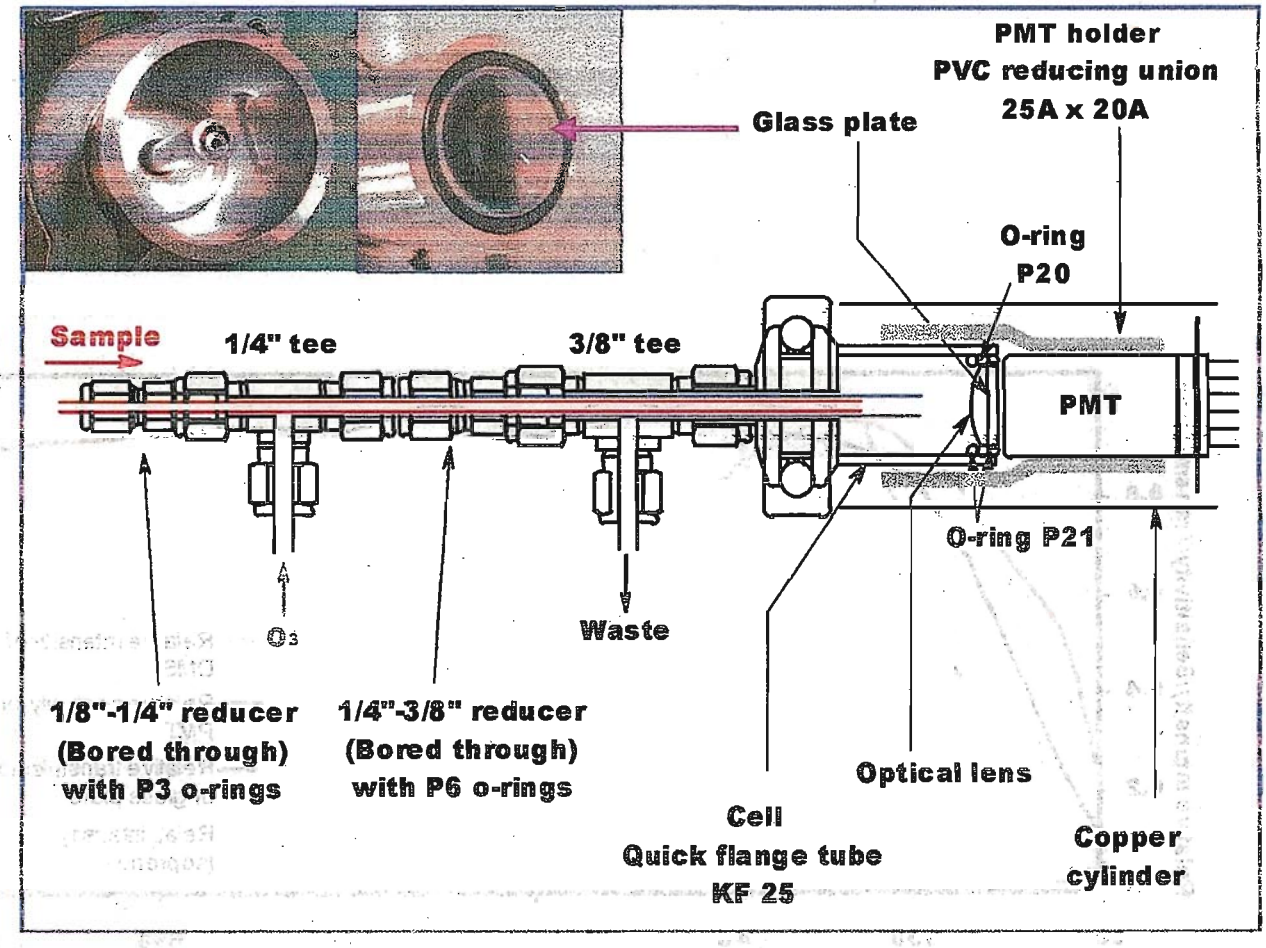

Figure 4.1. View of inside the reaction cell the reaction cell window , construction diagram of reaction cell and connection tubing. The 1/8" and 1/4" stainless steel tubes were fixed at the reducers with o-rings, so that positions of the tubes were adjustable. A small Teflon tube (AWG 24) was inserted in the entire 1/8" tube to minimize the volume between the trapping/separation column and the cell.

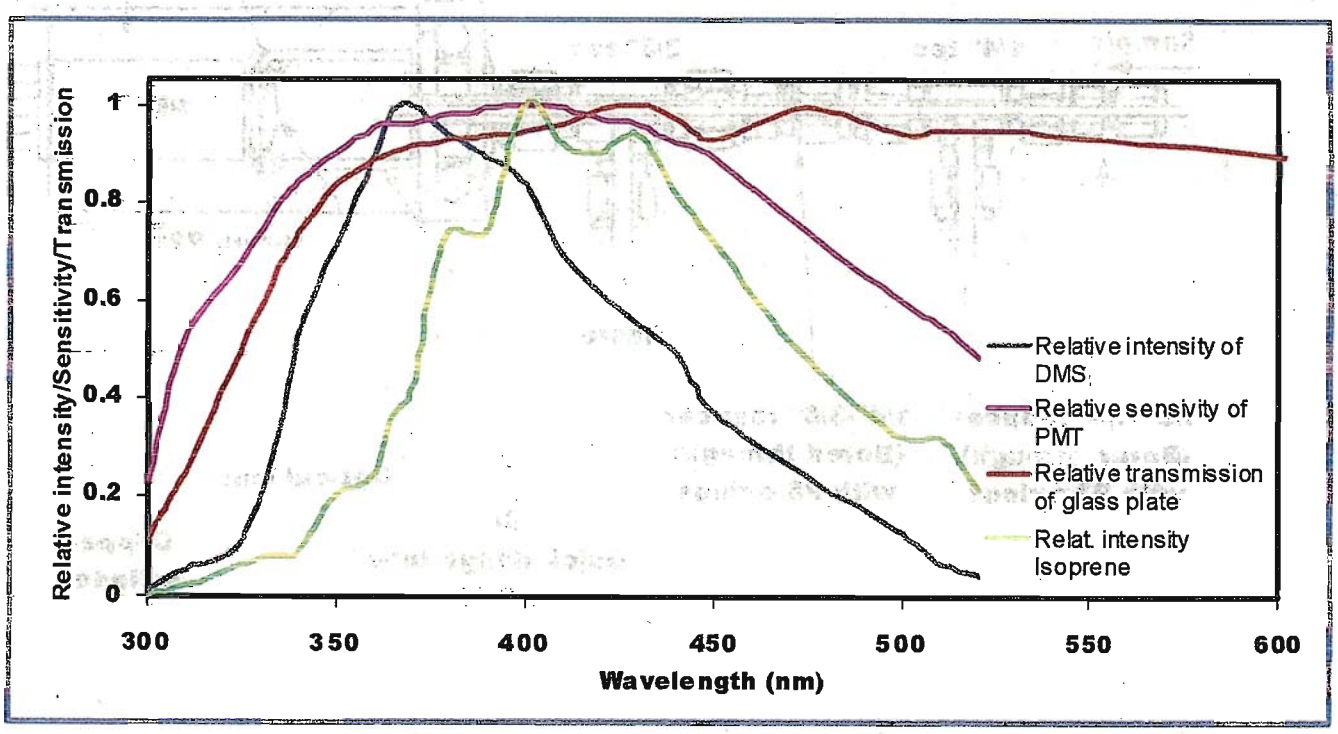

Figure 4.2. Relative sensitivity of PMT, relative transmission of the glass plate used at reaction cell window, relative emission spectra of DMS and Isoprene.

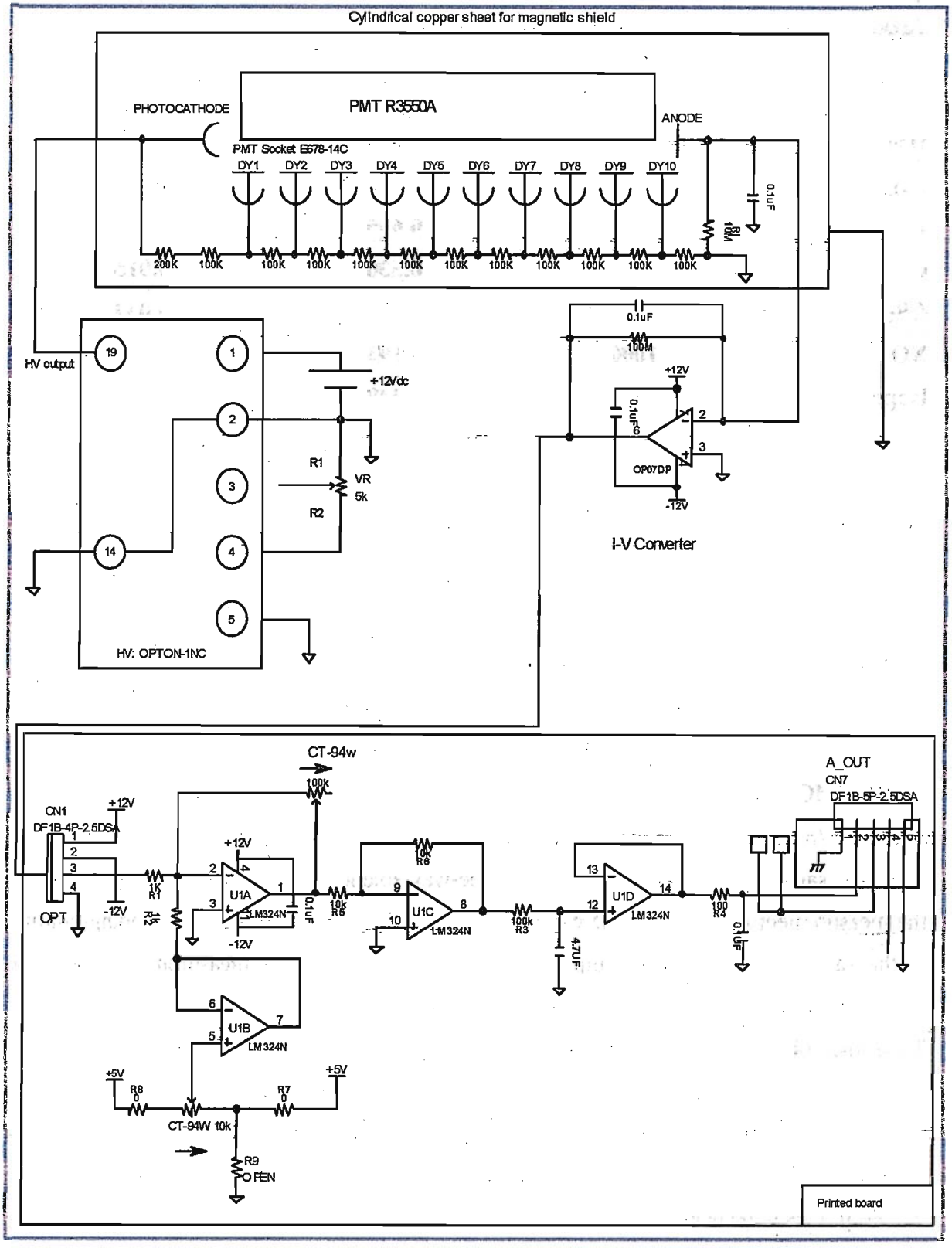

Figure 4.3. Circuit diagram of the PMT output signal processing and amplification.

Table 4.1. Sensitivity of the detector to common VSCs and compounds tested for interference normalized to DMS.

Compound	Conc. tested for sensitivity (ppbv)	Response (Volt)	Relative Response to DMS
DMS	10	3.455	1.000
CH_3SH	10	5.260	1.522
H_2S	50	0.695	0.040
COS	100	0.530	0.015
CS_2	100	1.175	0.034
NO	1000	0.193	5.594×10^{-4}
Isoprene	413	0.349	0.002

4.3.3. Instrumentation and Measurement Procedure

Measurements were performed using a system schematically shown in Figure 4.4. Sample was aspirated by a diaphragm pump (DA-55, ULVAC) and was normally by passed via a dummy column, DC1, which was filled with the silica gel as same as the trapping column to maintain the pressure constant in the flow system. When three-way solenoid valves (TV307'-6G-01, SMC, Tokyo, Japan) were activated, the sample passed through the trapping column at 200 mL/min, while the carrier gas (nitrogen) went through a dummy Teflon column, DC2. After the sampling (typically 5 min), the three-way solenoid valves were switched to go to the measurement mode where the carrier flowed at 25 mL/min through the trapping column in the same direction as the sampling. In the first 1 min of the measurement mode, the column temperature was kept at room temperature to remove the remaining air completely. Then, the column was heated to desire temperature stepwise at with constant carrier flow to purge the target gas to the chemiluminescence cell. The analyte gases were mixed with ozone flow (300 mL/min) in a tube–in–tube in the cell and chemiluminescence emitted was measured. After all gases were purged out, the column was cooled to be room temperature by two 8-cm fans to be ready it for the next measurement.

The ozone was prepared by passing air through an aluminum chamber at 300 mL/min where two ceramic electrode plates (w 25 mm x L 51 mm, 1100N (2501), Logy Electric, Tokyo, Japan) were settled. Pulse power was applied to the electrode from a control kit (LHV-9K-DC 12V, Logy Electric) to generate ozone in plasma. By using the two electrode

plates, 0.6% of ozone was generated at 300 mL/min air flow. The ozone containing waste gas was discharged through an ozone deactivating column.

The measurement was repeated automatically using two twin timers (H5CX from Omron, Kyoto, Japan). One of them was for solenoid valves (9 min OFF and 5 min ON) and the other was for the fans (14 min ON and 9 min OFF). When the cleaning of column at 320 °C was finished, alarm signal from the temperature controller reset the timers, and then column cooling started with the fans and constant carrier flow. After 9 min of cooling, the four solenoid valves were turned ON and 5 min of sampling started. Then, column flowing sample was taken back to the nitrogen carrier, and the fans were turned off. After 1 min purging with nitrogen, temperature was changed according to the programmed profile. When the final heating was completed, the temperature controller triggered the timers to reset for the next measurement cycle. See appendix 2 for details about instrument connection set up, temperature controlling program and operation cycle.

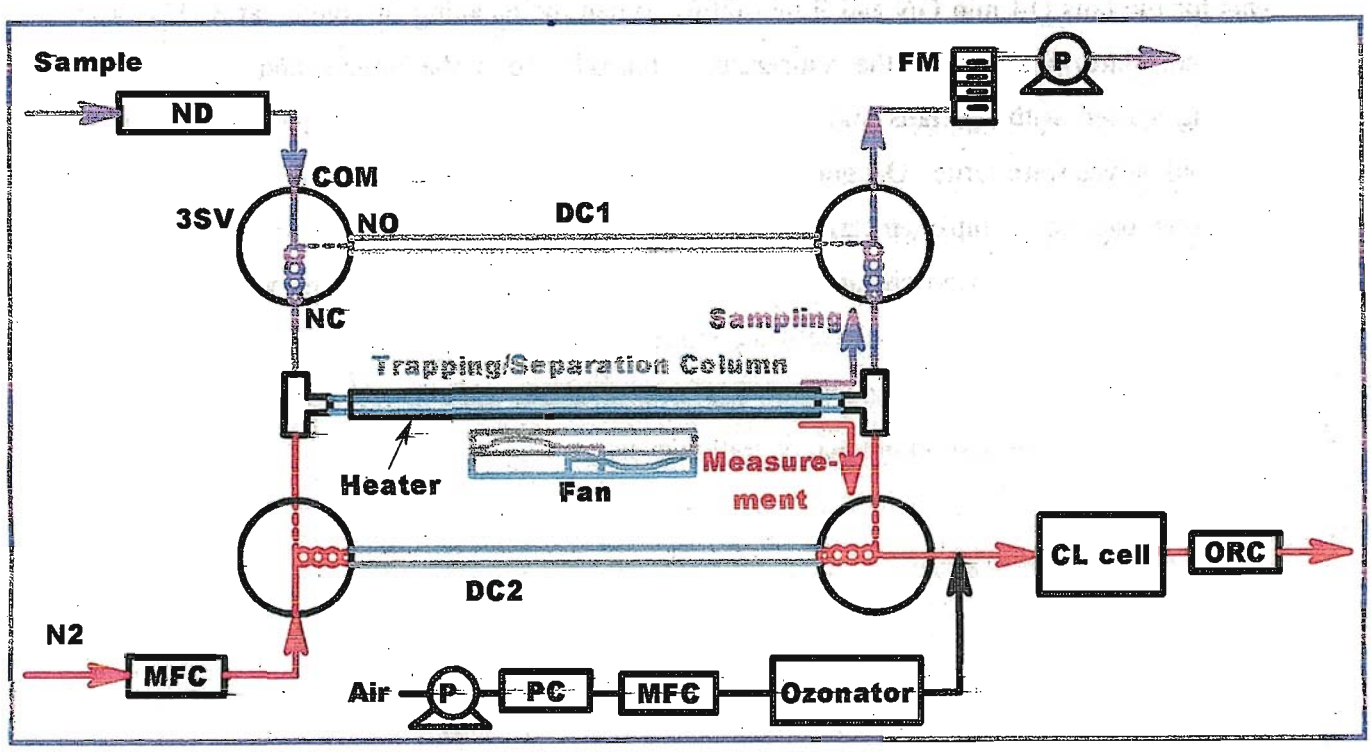

Figure 4.4. Flow diagram of the measurement system. ND: Nafion dryer, 3SV: three way solenoid valve, FM: flow meter, DC12: dummy columns, MFC: mass flow controller, PC: air purification column packed with sodalime and activated carbon, P: airpump, CL cell: chemiluminescence cell, ORC: ozone removing column.

4.3.4. Test Gas Preparation

The working gases (2~100 ppbv) were prepared from 100 ppm standard gases by dynamic dilution with purified air. The gas cylinder of H_2S, COS, CS_2 and CH_3SH were purchased from Sumitomo Seika Chemicals (Osaka, Japan) and DMS from Taiyo Nippon Sanso (Tokyo, Japan). The air was supplied by an oil-free compressor with dehumidifier (dry air supplier P4-EAD, Yaezaki Koatsu, Tokyo, Japan) and was further purified from water and organic compounds by the use of silica gel, sodalime and activated charcoal column.

The test gas of isoprene and DMS was produced by using permeation tube system. Some kinds of permeation tube was investigated for generation of DMS, isoprene and dimethyl disulfide (DMDS). The permeation apparatus was made up of a permeation chamber which contained permeation tube made by different types AWG (American Wire Gauge) Teflon tube and 1/8" or 1/4" PTFE Teflon tube. Flangeless nut with ferrule and cap (Upprich science) was used for AWG tube and 1/8" tube, swagelok cap with ferrule was used for 1/4" tube to make permeation tube. The permeation chamber was thermostated at 30 °C and a constant flow of dry, hydrocarbon-free air was passed through at a rate of 100 ml min^{-1}. The analyte flow could be further diluted to generate desired concentration of test gas. Table 4.2 Shows, preparation procedure and the characteristics of some permeation tubes. Figure 4.5, 4.6 and 4.7 shows that the representative permeation rate for isoprene, DMS and DMDS respectively. Theoretically, the life time of some permeation is several years. But in practical it was observed that the chemical became contaminated. Isoprene permeation tube could be use for 90 days and DMS, DMDS for more than 5 months.

Table 4.2.

Preparation procedure and characteristics of different types of permeation tube for DMS and isoprene (IP) and DMDS. Concentration with 100 ml min^{-1} air flow and theoretical life time.

Name of gas	Preparation procedure	Permeation window length	Permeation rate (µg/min)	Concentration (ppm)	Life time (Days)
DMS	Two pieces of PTFE tube (od 3.1mm x id 1.6mm x L 4.3cm) was inserted (head to head) in AWG10 tube (id 2.69mm x od 3.29mm x L4cm), one side of the each PTFE tube was closed by melting.	1 mm in AWG10 tube.	1.628	6.497	57
DMS	AWG11 Teflon tube (id2.41mm x od 3.01mm x L6.5 cm). One side was closed by melting and another side with Flangeless nut with cap.	5 cm	0.6919	2.761	248
DMS	1/4" PTFE tube (id 4.35mm x od 6.35mm x L5cm) with swgelok cap.	2 cm	0.1872	0.7506	2032
DMS	AWG10 Teflon tube (id 2.69mm x od 3.29mm x L6.5 cm). One side was closed by melting and in other side Flangeless nut with cap.	5 cm	0.8386	3.346	245
DMDS	do	7 cm	0.0986	0.235	2118
IP	1/4" PTFE tube (id 4.35mm x od 6.35mm x L5cm) with swgelok cap.	2 cm	0.1774	0.645	1592
IP	do	10 cm	0.4764	1.566	2930
IP	do	10 cm	0.4644	1.697	3011
IP	Two pieces of PFA tube (od 3.1mm x id 1.6mm x L 4.3cm) was inserted (head to head) in AWG10 tube (id 2.69mm x od 3.29mm x L4cm), one side of the each PFA tube was closed by melting.	1 mm in AWG10 tube	0.8748	2.877	38

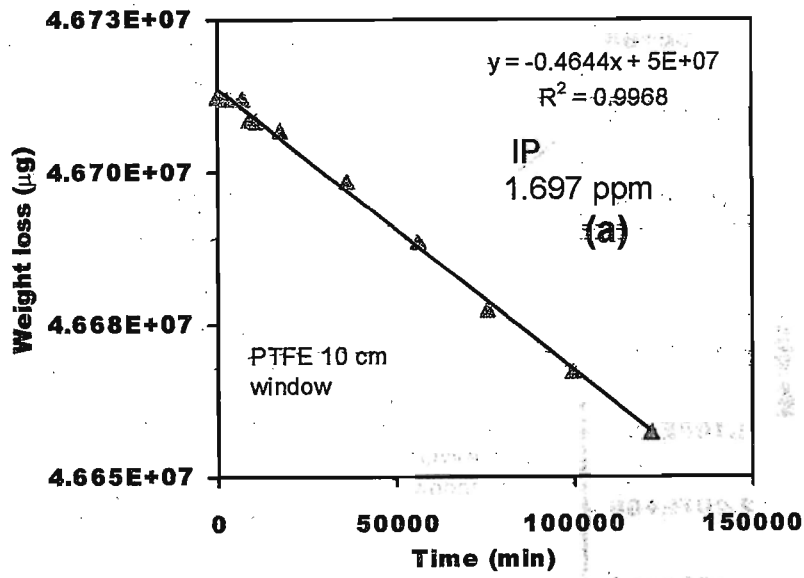

Figure 4.5. Permeation rate of isoprene permeation tube made by 1/4" Teflon (PTFE) tube with 10 cm permeation window. Concentration of isoprene was 1697 ppb for 100 ml min^{-1} air flow.

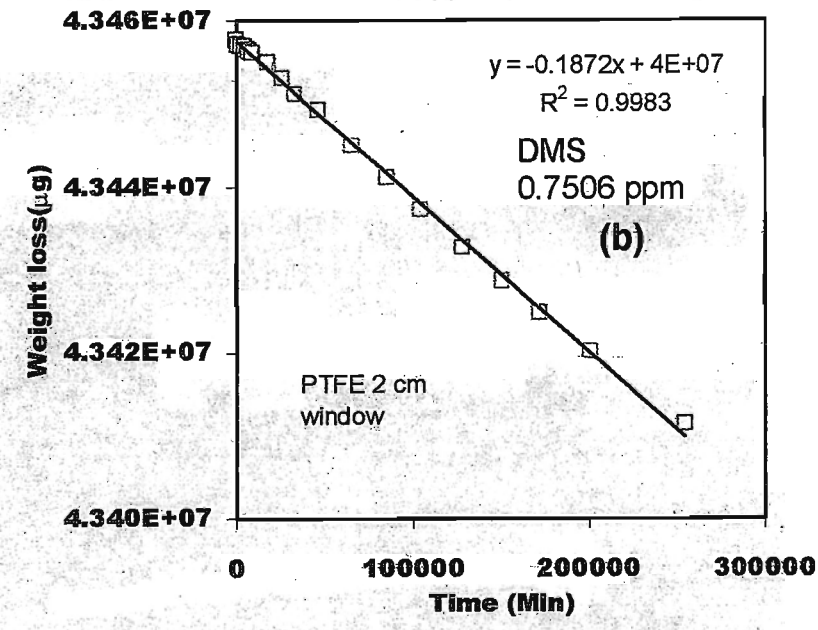

Figure 4.6. Permeation rate of DMS permeation tube made by 1/4" PTFE Teflon tube with 2 cm permeation window. Concentration of DMS was 0.7506 ppm with 100 ml min^{-1} air flow.

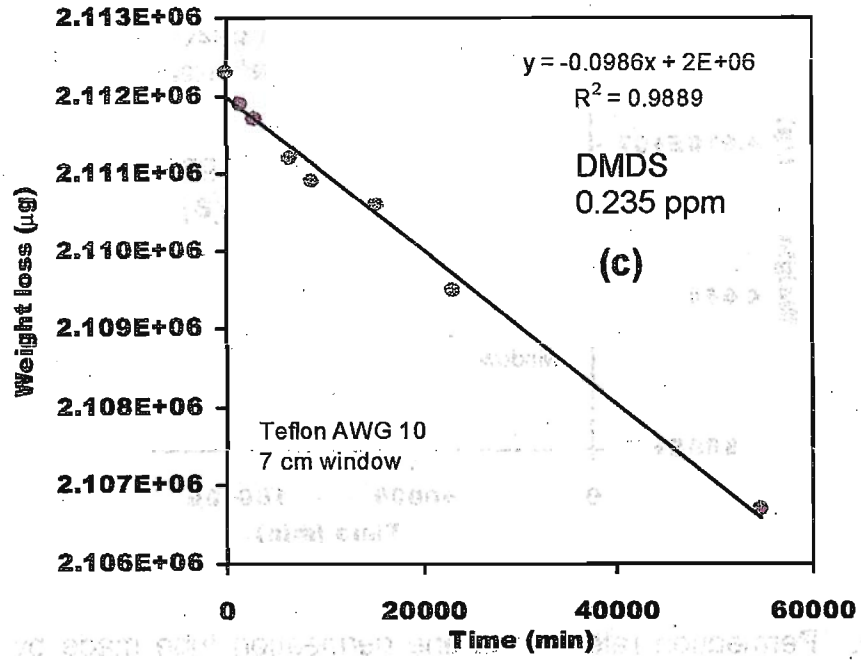

Figure 4.7. Permeation rate of DMDS permeation tube made by AWG 10 Teflon tube with (L8.5 cm x id2.69 mm x od3.29 mm) 7 cm permeation window. Concentration of isoprene was 0.235 ppm for 100 ml min^{-1} air flow.

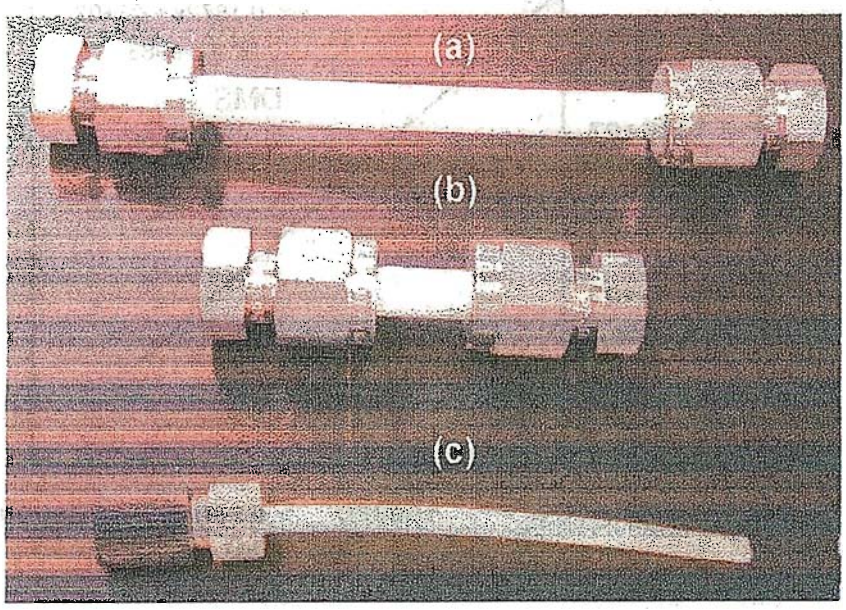

Figure 4.8. Pictures of different type permeation tube investigated for isporene. Picture (a) and (b) are 1/4 inch PTFE Teflon tube and (c) is AWG10 Teflon tube.

4.3.5. Sample Measurements

Human breath and headspace of septic tank were analyzed by the present system. A Nafion dryer was placed at the sample inlet to remove water vapor from the real samples. Breath samples and headspace gases of a septic tank were collected into 5 L cleaned Tedlar bags. In case of breath sampling, a column (10.8 mm id x 75 mm L) packed with calcium chloride was placed in front of the Tedlar bag inlet to reduce water vapor. The sampled breath and septic tank airs were then measured by the present system three times each.

Diurnal variation of the gases was examined in a toilet room. All parts were settled in an aluminum box. AC power was obtained from a wall socket in the toilet. Nitrogen packed in a 1-L can was used in short measurements. When the measurements were longer than 3 h, 10 L gas cylinder was used. The measurement was repeated automatically by using the programmable temperature controller and the timers. All data was acquired with a data logger.

4.3.6. Comparable Measurements with GC-FPD

The above samples were also measured by GC-FPD coupled with the trap/desorption system concurrently with the present method for the validation. A Tenax TA column was placed in a dry ice-methanol bath,[11] and the sample from the Tedlar bag was trapped at 50 mL/min for 10 min into the Tenax column, and then purged with helium for 1 min. Next, the bath was exchanged to hot water bath (90 °C) to warm the column for 30 sec, and then the desorbed gases were introduced into GC system. Separation was carried out with a Teflon column (id 2.36 mm x od 3.18 mm x 3 m) packed with *β,β'*-ODPN, Uniport HP 60/80 mesh. Gas chromatograph used was Shimadzu 14A with the carrier gas helium at 20 mL/min. Also hydrogen (60 mL/min) and compressed air (40 mL/min) were used for the detector flame.

4.4. Results and Discussion

4.4.1. Chemiluminescence Reaction Cell

A simple reaction cell was designed and constructed to detect CH_3SH and DMS with high sensitivity. There was no machined block and the cell was light, simple, cheap and easy to construct. The cell was made with mirror-finished stainless steel tube which volume was 20 or 10 ml. The sample with carrier gas and ozone were introduced into the cell through concentric tubes where ozone came via the outer tube. Substantial chemiluminescence intensity variation was observed with changes in sample/carrier-ozone flow rates and the gas inlet tube positions in the reaction cell. Optimum chemiluminescence intensity with

minimum noise was observed at 25 mL/min sample/carrier flow rate. The chemiluminescence intensity was not significantly influenced by gas inlet tube's position in the reaction cell but it was worthwhile for minimization of signal noise. The 1/4" tube was positioned at 10 mm away from the optical lens, and the 1/8" tube was 10 mm upstream from the end point, inside the 1/4" tube. 300 mL/min ozone flow rate was found optimum for maximum chemiluminescence intensity. Air was better than oxygen for the ozone source. When air is used in the ozonizer instead of oxygen, trace level NO_x is generated in the ozone stream and enhanced the chemiluminescence reaction.[29]

4.4.2. Mini-Column for Trap and Separation

The VSCs levels in air are usually too low for direct determination. Therefore, a preconcentration and isolation step must be included in the analytical method. These steps were performed only with one column in this system. Solid adsorbents were packed in a ceramic tube (Mullite) for both preconccentration and separation of the gases. Mullite tube has higher thermal conductivity (5.0 W/(m K)) than that of glass tube (1.1 W/(m K)) and resistance to chemical attack over the maximum temperature range of this investigation (330 °C). The availability of thin wall ceramic tube enabled us to make column with small heat capacity. This is important for rapid temperature control and low power consumption. Good temperature profile in the whole effective area of the column was obtained. The surface temperature of the column was constant within +/- 5 °C at 300 °C.

In this study, cryogenic trapping was avoided to reduce the experimental complexity. Some kinds of solid adsorbents were examined at ambient condition with single or multiple beds of adsorbents to trap the sulfur gases; e.g. silicagel, molecular sieve, carbosieve S III, Tenax TA, and activated charcoal. The adsorbents were investigated in the view of trapping efficiency and separating ability of gases according to the desorption temperature of the gases. Clean air, and nitrogen was investigates as a carrier. It was observed that the sensitivity was significantly decreased when air was used as carrier. Reduced sulfur gases might oxidize with air as carrier. Beside that, when air was used as carrier, the trapping efficiency of the adsorbents was low and the desorption temperature was not stable. Figure 4.9 shows that the desorption temperature and the type of adsorbent investigated. According to our investigation and also previous report silicagel was the most suitable adsorbents regarding not only trapping efficiency[42] but also separating ability. In the present study, the key factor of the gas separation was selective elution of the gases from the adsorbent according to their desorption temperature. The gases are adsorbed on the silicagel surface by

molecular attraction such as van der Waals interaction. In general, the attraction becomes higher with increase in molecular size, and every gas has specific desorption temperature on a specific adsorbent. Accordingly, the smaller molecule would desorp at lower temperature.

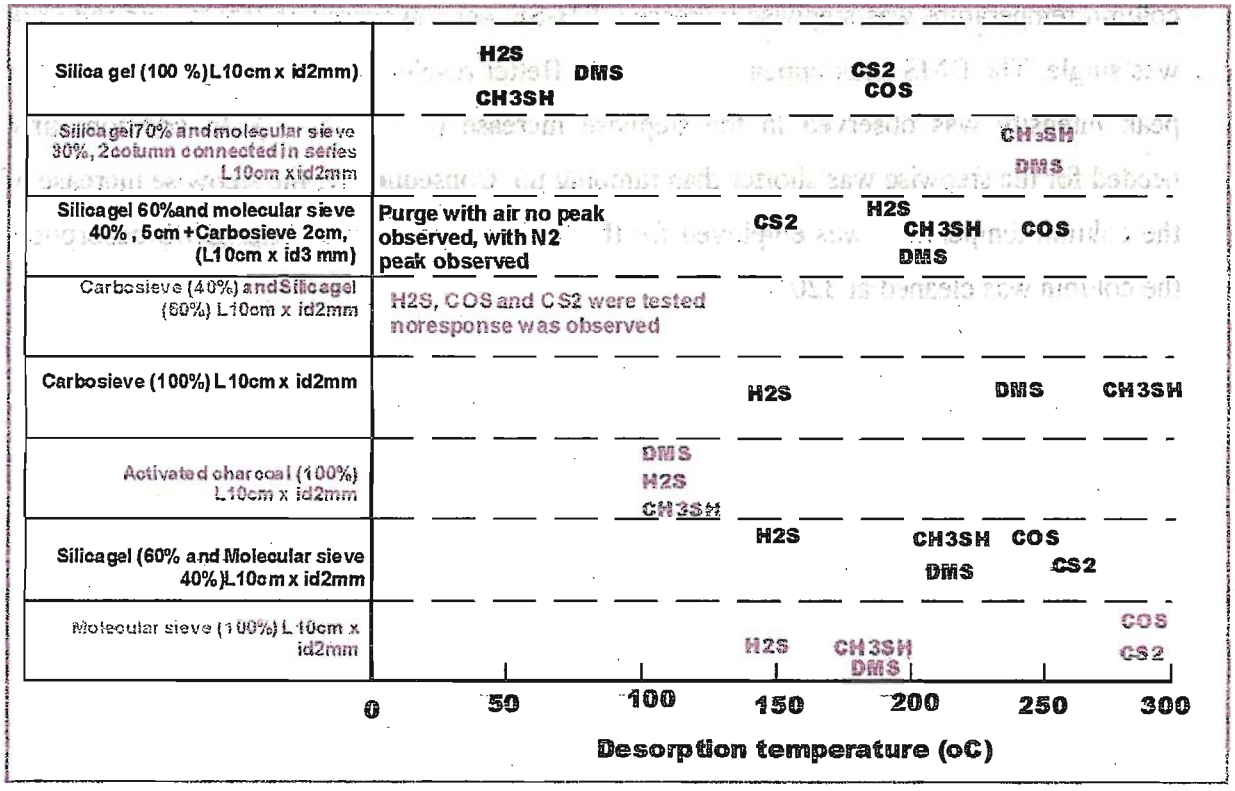

Figure 4.9. Adsorbent column type and desorption temperature of reduced sulfur gases when air was used as carrier.

In this work, the simple principle was employed for the gas separation. Temperature of the gas-trapping column was ramped up with keeping the continuous carrier flow. The gases were eluted according to the desorption temperature of gases and detected followed by chemiluminescence reaction. The gas separation was investigated with ramping up and stepwise increase of the column temperature. Figure 4.10 represents chromatograms obtained with the two methods after trapping of 8 ppbv of CH_3SH and DMS for 5 min. While temperature of the column increased at constant rate 42°C/min, peaks appeared around 160°C and 240°C for CH_3SH and DMS, respectively. In chromatogram (Figure 4.10a), we can see there was a small peak between CH_3SH and DMS peak around 180°C.

The small peak was recognized as CH_3SH by examining with CH_3SH and DMS separately. CH_3SH molecule have smaller critical diameter (4.5 Å) than that of DMS and supposed to enter easily into the cavity of porous silicagel. Reason of the two peaks for CH_3SH might be that a fraction of CH_3SH molecules retained within the internal cavities of silicagel to desorb at higher temperature (180 °C) than the normal desorption temperature. When the column temperature was stepwise increased, CH_3SH peak appeared at 190 °C and the peak was single. The DMS peak appeared at 270 °C. Better resolution between peaks and higher peak intensity was observed in the stepwise increase (Figure 4.10b). In addition, time needed for the stepwise was shorter than ramping up. Consequently, the stepwise increase of the column temperature was employed for the further experiments. After DMS desorption, the column was cleaned at 320 °C.

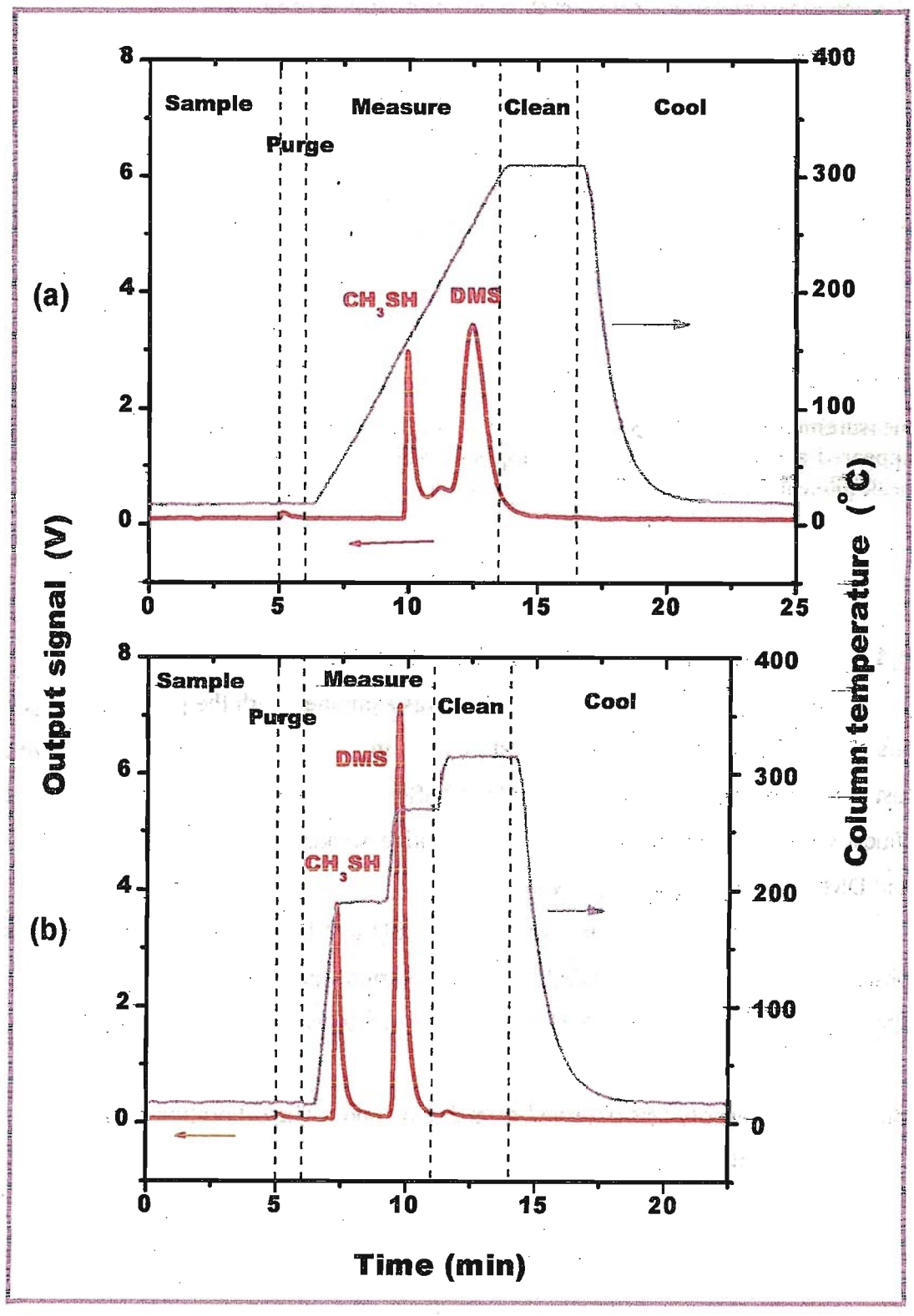

Figure 4.10. Effect of column temperature increasing pattern on response of gases.

Table 4.3.
Chemiluminescence characteristics of sulfur gases

Name of gas	Desorption temp. (°C)*	Concentration (ppb)	Response (V)**	Relative response
DMS	240	10	3.11	1.00
CH_3SH	160	10	2.40	0.773
H_2S	150	10	0.0294	0.0094
COS	150[a]	10	0.0380	0.0122
CS_2	150[a]	20	0.522	0.0839
NO	150	100	ND	0
Isoprene	180	185	0.748	0.0117

*Desorption temperature was determined from trap/purge system and single gas measurement. [a]When COS and CS_2 measured mixed with CH_3SH and DMS the peak was appeared at 100 °C. measured** Response intensity was determined by corresponding peak intensity measured by trap/purge system

4.4.3. Performance of the Measurement System

The performance of the present method was examined with the prepared test gases. The first 5 and the last 5 chromatograms are shown in Figure 4.11 shows the first five and the last five chromatograms when 10 ppbv CH_3SH and DMS measurement was repeated 20 times. Good repeatability was obtained. Relative standard deviations for 10 ppbv CH_3SH and DMS were 3.2% and 1.9%, respectively.

Figure 4.12 shows calibration curves for CH_3SH and DMS. Linear calibration plots were observed from 2 to 100 ppbv CH_3SH. The calibration equation was

PMT signal (Volt) = 0.8634 × CH_3SH (ppbv) − 2.2992 with r^2 value of 0.9987

But for DMS linearity was observed from 2 to 60 ppbv. The calibration equation was

PMT signal (Volt) = 0.8634 × CH_3SH (ppbv) − 1.2328 with r^2 value of 0.9994

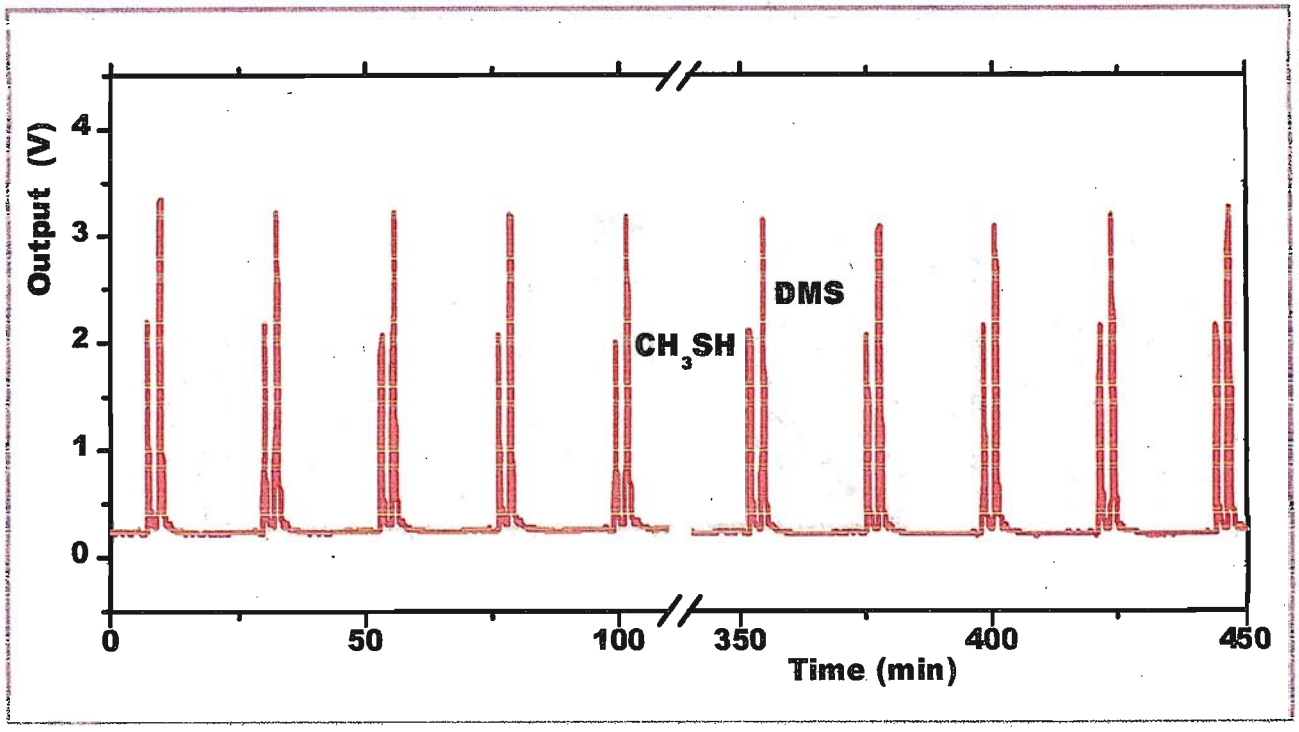

Figure 4.11. Chromatogram of standard gas mixture measured by the present system for 10 ppbv CH_3SH and DMS obtained with the shorter (20 mm) cell.

It was observed that DMS saturates the detector at concentration above 60 ppbv. The nonlinearity of DMS calibration plots over 60 ppbv wasn't clear but the possible reason might be less reactivity of DMS to ozone than that of CH_3SH. Kelly et al.[29] reported that the cause of nonlinearity in the calibration plot may result from a heterogeneous processes in the sulfide oxidation. Limits of detection corresponding to three times the blank signal deviation were 0.3 ppbv for CH_3SH and 0.05 ppbv for DMS.

As shown in Figure 4.12, the calibration curves are basically linear in the measurement range.[29] This is one of merits of the chemiluminescence method. In case of FPD, the main light emitting species is S_2* and the light intensity is proportional to square of the analyte concentration as well known. On the other hand, the analyte generally becomes SO by the reaction with ozone, and then SO_2* is formed by the second reaction with ozone.[40]

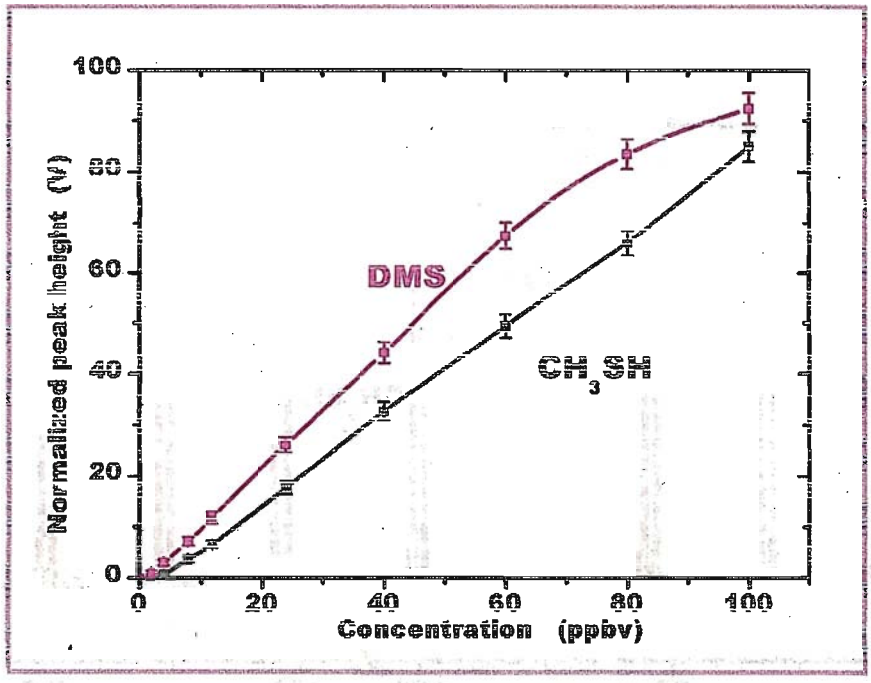

Figure 4.12. Calibration curve for CH_3SH and DMS measured by the present system.

4.4.4. Interference from other Gases

Interference from other gases was examined. NO is known as the chemiluminescence emitter, and the most popular NO analyzer is based on the chemiluminescence by the reaction with ozone. As shown in Table 4.2, however, there is no effect from NO. The NO chemiluminescence is centered at 1200 nm and starts from 600 nm.[43] The PMT used did not respond to the light over 650 nm and very poor signal was obtained even at 1000 ppbv of NO in direct measurement. In the trap/separation and chemiluminescence detection system, recognizable signal was not observed for 100 ppbv NO even in the high sensitivity mode.

Olefins are the compounds that may interfere with selectivity towards reduced sulfur compounds, on the order of a thousand to one.[32] Potential interference from isoprene was investigated, because considerable amount of isoprene is present in human breath. The chemiluminescence of isoprene was three order less than DMS intensity in the direct chemiluminescence measurement. When isoprene (prepared from permeation tube) was measured by the present trap/separation system, desorption temperature was near for CH_3SH but considerable peak was not observed.

Since COS and CS_2 chemiluminescence intensities observed were low compared to DMS intensity. In real-world monitoring environment, they are not present in significant amount and have less potentiality to interfere with CH_3SH detection. Desorption temperature of COS and CS_2 were 90 and 100 °C in the ramping up system and much lower

than CH_3SH. When the column was stepwise increased, CS_2 peak appeared very quickly at 190 °C and could be distinguished from the CH_3SH peak.

One of the major sulfur gases, H_2S, desorbed from silica gel around 150 °C, which was close to CH_3SH desorption temperature. Therefore it was difficult to separate H_2S and CH_3SH. Fortunately, the chemiluminescence signal of H_2S was much smaller than that of CH_3SH. Furthermore, the recovery of H_2S in the silica gel trap system was poor because of high volatility and reactivity. Accordingly, in the trap/separation and chemiluminescence system, the H_2S signal was only 1/100 of that of CH_3SH. There is no need to concern for H_2S interference on the CH_3SH determination in the normal odor analysis. If H_2S level was much higher than CH_3SH (more than twenty times), the H_2S interference may be concerned. In that case, H_2S could be selectively eliminated by used a small column (16 mm id x 10 cm) packed with glass wool treated with 5% Na_2CO_3/5% glycerin, which was placed at the downstream of the Nafion dryer.

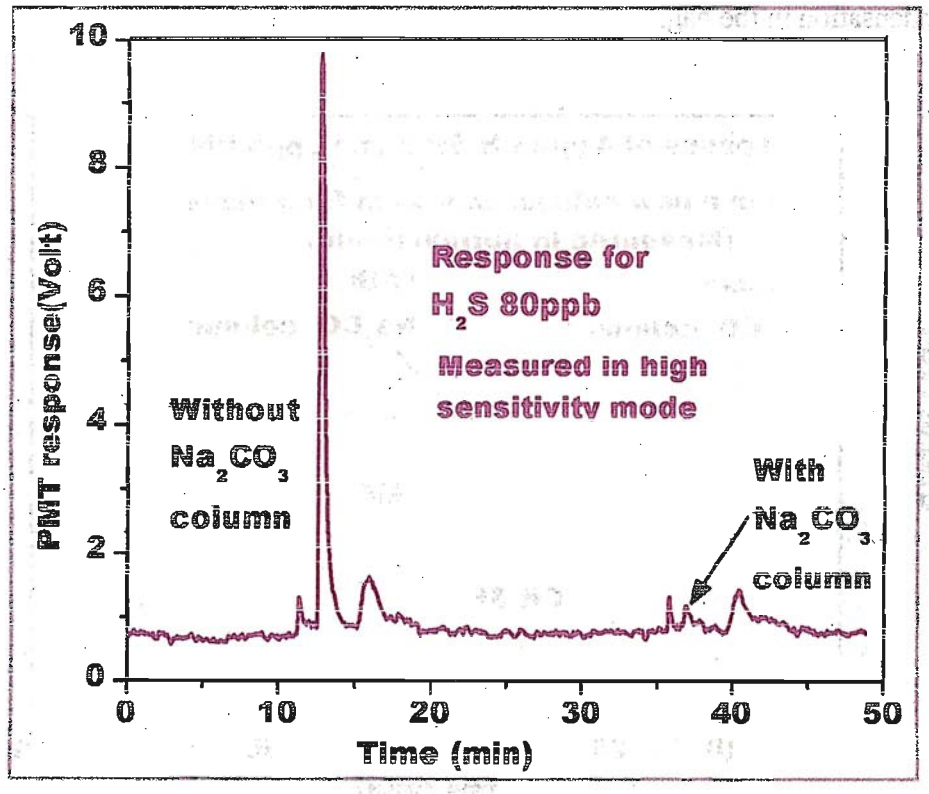

Figure 4.13. Effect of Na_2CO_3 column to remove H_2S from sample stream. The peak height with sodium carbonate column was equal to the blank peak height.

The column was tested with 200 ml min^{-1} sampling rate and 80 ppb H_2S concentration. Figure 4.13 shows that the column was effective to remove H_2S from sample stream. The column was found active after used for over 50 samples measurement.

The effect of sodium carbonate column on sensitivity of CH_3SH and DMS was also investigated. Response of these two gases measured with and without column shows that DMS sensitivity was not affected by the column. But CH_3SH sensitivity was affected by a new column. When first measurement was performed with new column, sensitivity became decreased up to 50% of measurement performed without column (Figure 4.14). Sensitive of CH_3SH was increased and became stable within $2^{nd}/3^{rd}$ measurement. The new Na_2CO_3 column may also have some adsorption site for CH_3SH and become saturated within $2^{nd}/3^{rd}$ measurement.

The recovery of the both gases was affected by the humidity of sample. Peak intensity of CH_3SH was significantly reduced (40-50 %) for highly humid sample, whereas DMS peak was reduced 10-20 %. Therefore, a Nafion dryer[3,44-46] as used during trapping the gases. In our examination, the loss of CH_3SH and DMS in the Nafion dryer was negligible. In case of breath sampling, the air was pre-dehumidified through a calcium chloride tube to prevent water condensation in the bag.

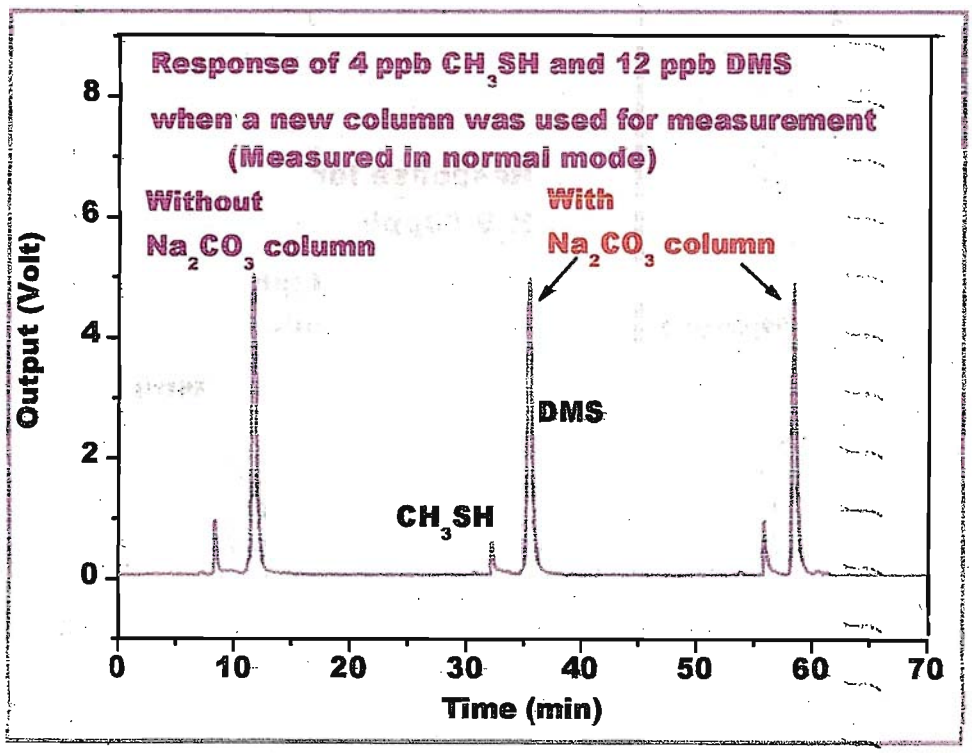

Figure 4.14. Effect of Na_2CO_3 column on measurement of CH_3SH and DMS. Response of gases, when first and second measurement was performed with new column.

4.4.5. Application to Breath Odor and Septic Tank Headspace Gas Analysis

Human breath samples and headspace sample of a septic tank were measured by the single column trapping/separation method. Some samples were simultaneously measured by cryogenic trap GC-FPD system to validate the present system. Data shown in Table 4.5 are concentrations of CH_3SH and DMS contained in breath and septic tank samples obtained by the both methods. Figure 4.15 shows that the representative chromatogram of breath sample measurement with Na_2CO_3 column in the sampling line. The data obtained by the two methods mostly agreed well each other. But some of the breath could not be measured by GC-FPD. For examples, breath F and G contained low DMS and not suitable for GC-FPD. The gas levels of breath samples H and K were not low in the present method, but they were not detected in GC-FPD. Interestingly, they were tobacco smoker and probably the sulfur gases reacted with tobacco ingredients to disappear in the trapping column. The cryogenic trapping used in the GC-FPD method was supposed to collect many kinds of gases. We originally used 2 min heating for desorption as reported[37,41] however some breath gave no peak at that time. When the warming was shortened to 30 s, the peak was obtained even for these samples. The breath measurement using cryo trapping seemed difficult. On the other hand, silica gel does not retained the reactive compounds at room temperature and reliability is supposed to be better.

A discrimination of data was observed in case of CH_3SH concentration in headspace sample, GC-FPD system was unable to detect low-level CH_3SH. The septic tank sample did not content much high level of sulfur gases probably due to the cold season. In contrast to the breath air, DMS was richer than CH_3SH in the septic tank. CS_2 in the septic tank was relatively high and CS_2 peak was observed just before CH_3SH peak in the present method. The peak height corresponded to 10 ppb. The trap/separation and chemiluminescence instrument was easy to operate, more sensitive and had less effect from contaminations. The two major odorous compounds successfully measured by the present instrument.

Table 4.4.
GC-FPD instrument and measurement condition

Instrument	GC-FPD, Shimadzu 14A
Separation Column	Teflon tube L2 m x id2.36 mm x od 3.18; ODPN 60/80 mesh; each end of the column was plugged with glass wool.
Carrier gas	Helium 20 ml min^{-1}
Column temperature	70 °C
Detector temperature	120 °C
Hydrogen	40 ml min^{-1}
Air	60 ml min^{-1}
Trapping column	U-shaped teflon column (L35 cm x id2.36 mm x od3.18 mm) filled with Tenax TA 60/80 mesh 11cm bed, cooled in dry ice-methanol mixture
Desorption temperature	90 °C water bath
Sampling rate	50 ml min^{-1}

Table 4.5.
Measurement of breath and headspace of septic tank samples by the present trap/separation chemiluminescence system and GC–FPD system

Sample Breath (sex, age)	Sampling date	CL system		GC-FPD*	
		CH_3SH	DMS	CH_3SH	DMS
A M, 31	Jan. 27, 13:30	13.2 ± 0.0	18.8 ± 0.6	12.9 ± 0.3	23.2 ± 0.3
B M, 45	Jan. 27, 18:30	26.3 ± 2.1	9.23± 0.49	28.8 ± 0.0	7.75± 0.28
C F, 23	Jan. 30, 14:00	9.57± 0.10	9.14± 0.29	9.64± 0.69	9.30± 0.72
D F, 24	Jan. 31, 18:00	13.2 + 0.3	5.07± 0.15	10.5 ± 0.39	4.83± 0.24
E M, 28	Jan. 31, 12:30	10.1 ± 0.6	7.13± 0.25	8.50± 0.10	6.85± 0.19
F F, 22	Jan. 30, 18:30	7.52± 0.49	1.75± 0.22	ND	ND
G M, 56	Jan. 31, 12:30	6.16± 0.15	3.37± 0.01	ND	ND
H M, 28, smoker	Jan. 30, 17:30	11.2 ± 0.72	2.60± 0.15	ND	ND
K M, 26, smoker	Jan. 31, 11:00	18.2 ± 0.4	11.4 ± 0.07	ND	ND
Headspace					
Septic tank 1	Jan. 27, 15:30	2.30± 0.14	11.6 ± 0.7	ND	11.0 ± 0.6
Septic tank 2	Jan. 31, 17:30	1.12± 0.10	11.1 ± 0.8	ND	9.80± 0.48

* The LODs of GC-FPD measured gases were CH_3SH 2.4 ppbv and DMS 2.1 ppbv.

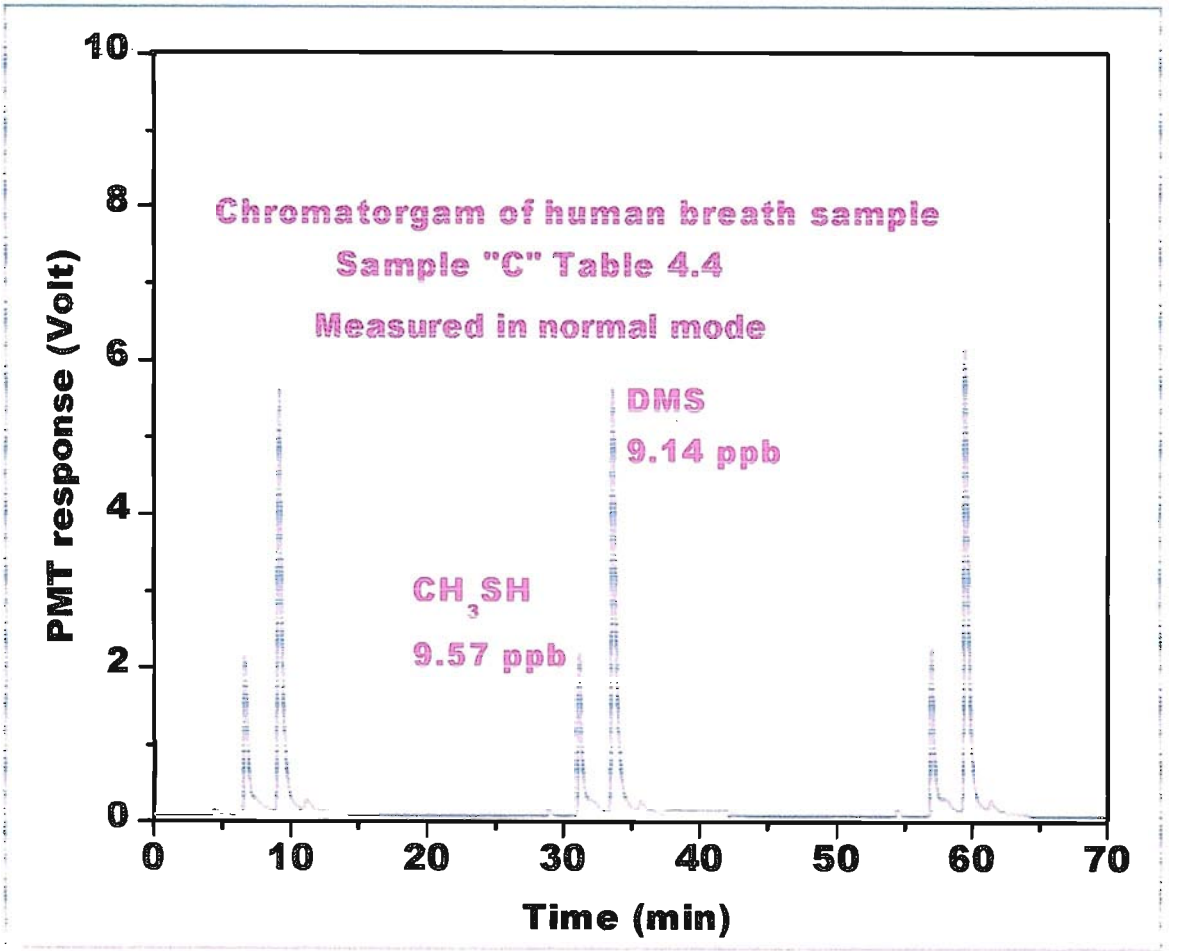

Figure 4.15. Representative chromatogram of human breath sample.

4.4.6. Automated Measurements of Toilet Air and Emission from Tidal Flat Sediment

The present instrument is suitable not only for batch wise measurement but also semi-continuous automated measurement. The instrument was brought to a toilet room and on-site air analysis was performed for three days. The measurements were automatically repeated 220 times. The sensitivity of the instrument was checked with the standard gases before and after the campaign, and the responses were quite same within 10%. The same trapping/separation column could be used for three days. H_2S level was also measured simultaneously in the last day of the campaign by micro gas analysis system (μGAS).[36] Figure 4.16 shows the concentration of the gases in the toilet air during the measurement period. CH_3SH was in ppbvs and DMS and H_2S were in sub-ppbvs. The gas levels were lower than expected. The campaign was performed in late-winter during which microorganism activity supposed to be low. Furthermore, during the campaign, only few people used the toilet because the campaign was conducted during the spring vacation. During the measurement period very low smell of the toilet substantiated the low level of gas concentration. Even in such situation, the odorous sulfur gases could be measured and daily variation was obtained. Interestingly, the both gas levels drastically increased after became dark. The gas levels reached at maximum in the early evening everyday. After the evening, it was decreased gradually to the normal level: it seemed that was due to the sulfur source exhausted within a few hours. Before leaving their work place around 6-7 PM people might frequently used the toilet and the gas level became at maximum. Compared to CH_3SH, DMS retained relatively long time. This suggested that the lifetime of DMS was longer than that of CH_3SH. Generation of sulfur gases in the nighttime is reported in some literatures[6,38] but detail of mechanism is not clear at this time. The instrument presented here may help the investigation of gas emissions. The toilet air also measured in summer June 5-10, 2006 at Kumamoto University. Figure 17a shows that the concentration level was lower than that of March, 2006 measurement but the concentration variation pattern was similar.

Marine tidal sediment is well known for emission of reduced sulfur gases to the atmosphere, especially DMS. The applicability of the present instrument was investigated for emission from the sediment. Marine sediment sample was collected from muddy tidal flat of Ariake Sea at Sumiyoshi in June 12, 2006. The sample was collected in a box (30 cm w x 26 cm d x 16 cm h) without disturbing the surface of the sediment and brought to the laboratory. The emission was measured according to the sampling procedure described in section 2.3.4. CH_3SH and DMS were measured by the present system and H_2S was

measured by μGAS. The emission was simultaneously and automatically measured during June 12-17, 2006. Figure 4.17b shows the emission rate of sulfur as H_2S, CH_3SH and DMS with total sampling rate of 600 mL/min (400 mL/min for μGAS and 200 mL/min for present system). The data in Figure 4.17b shows that emission flux of CH_3SH and DMS was increased at noon during 13-15 June while H_2S emission was remain almost constant. The cause of highest emission variability of DMS among these gases might low solubility in water. The variability of emission fluxes might result of increasing the temperature at daytime. From June 16 emissions of three gases were increased simultaneously might due to drying up the soil surface.

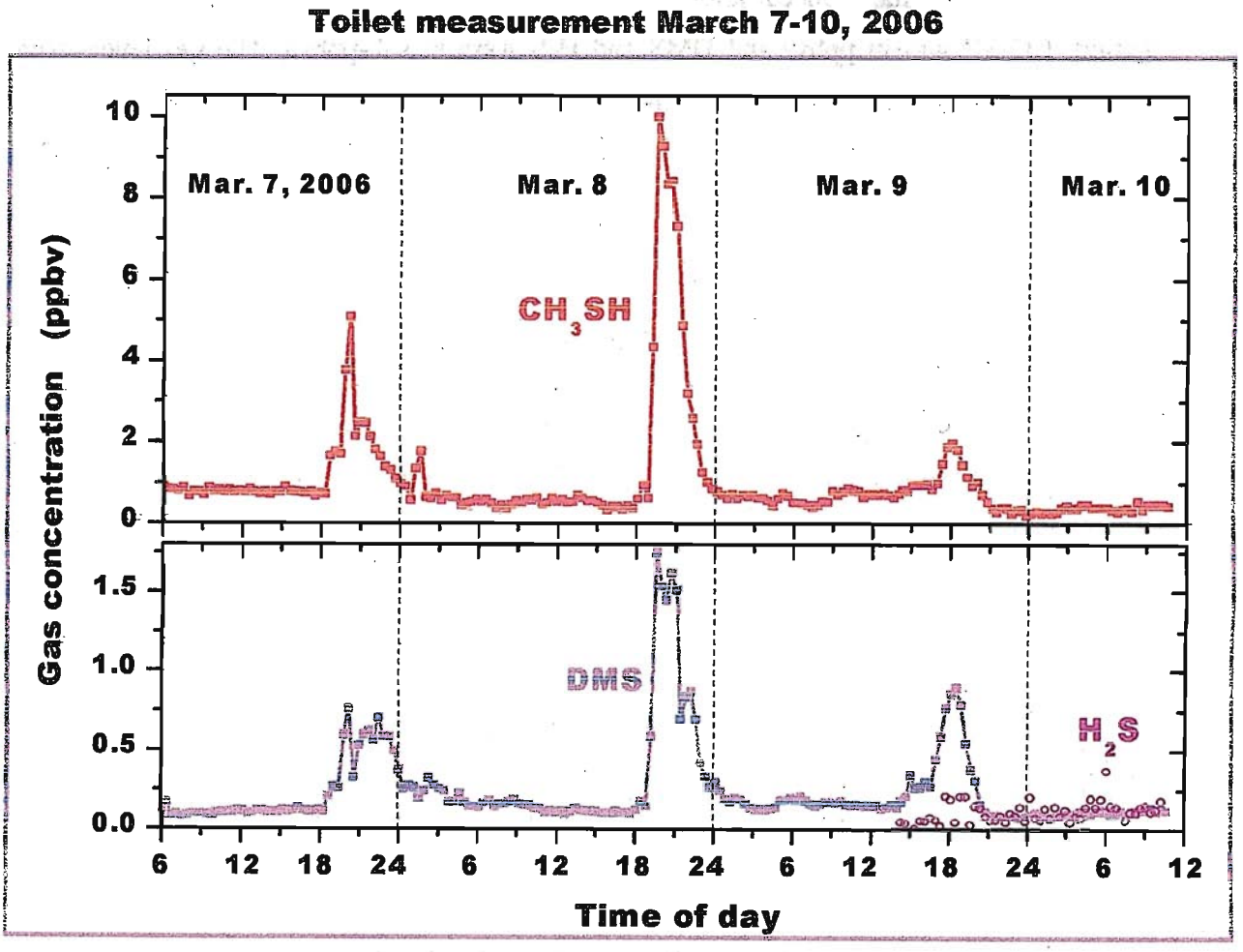

Figure 4.16. Trend of CH_3SH and DMS levels in a toilet air in winter. The gases were measured three days in the rest room. Also H_2S was measured on the last day by μGAS.

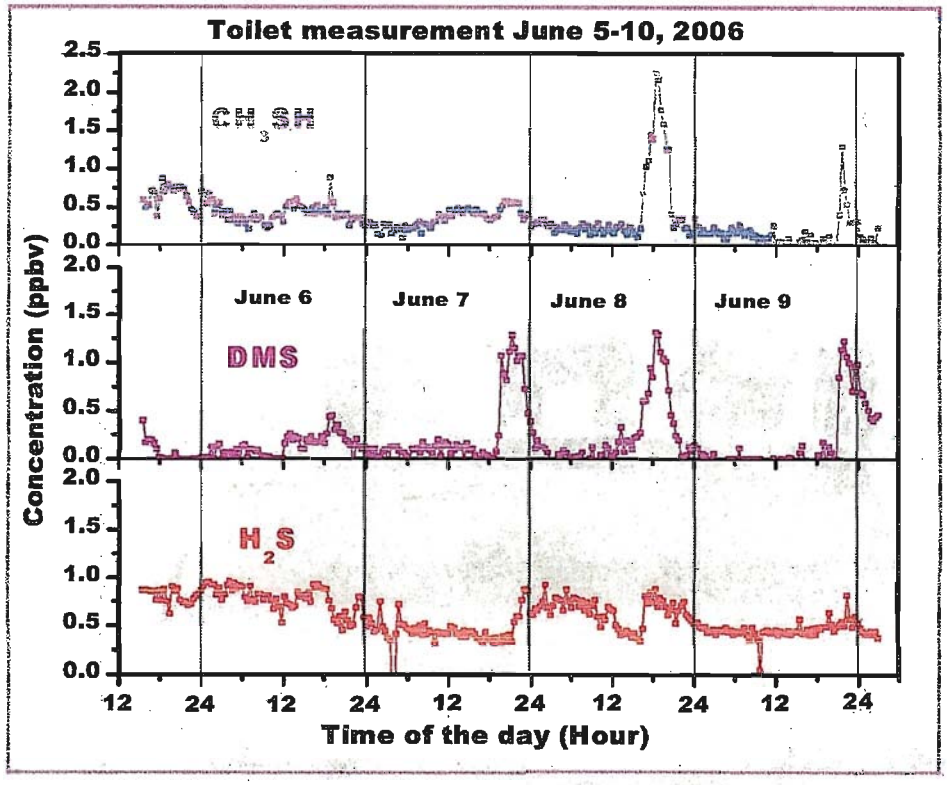

Figure 4.17 (a). Trend of CH_3SH and DMS levels in a toilet air in summer.

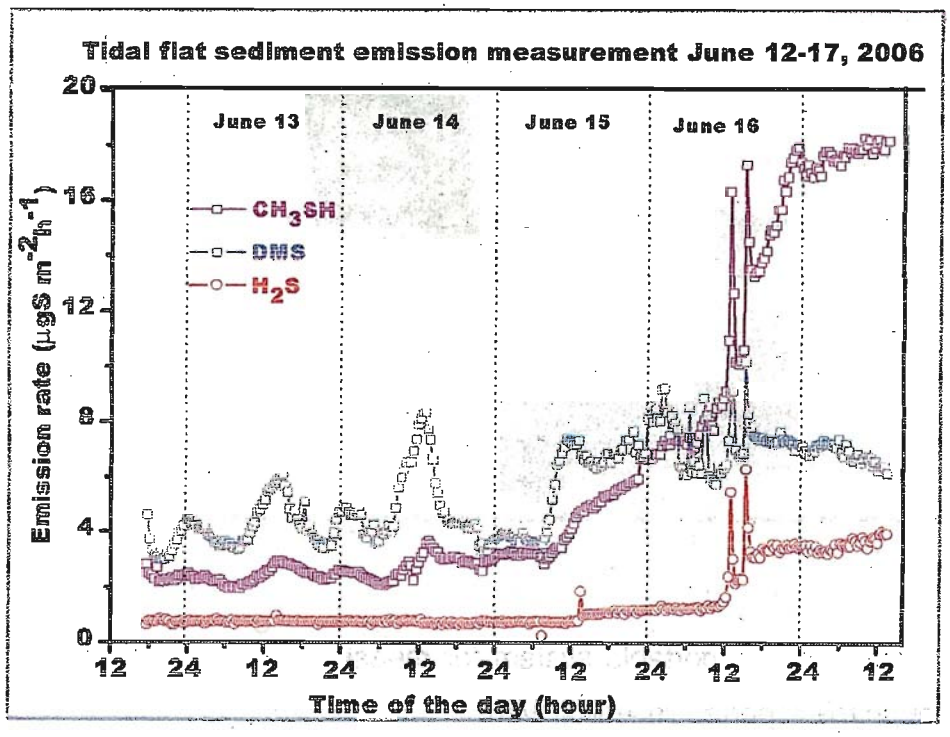

Figure 4.17 (b). Trend of CH_3SH, DMS and H_2S emission from collected marine sediment to the atmosphere during June 12 to 17 measured in the laboratory. CH_3SH and DMS were measured by present system and H_2S was measured by μGAS. The gases were measured three days in the rest room

Figure 4.18. Picture of the portable system for measurement of CH_3SH and DMS developed through the reported research work.

4.5. Conclusion

A simple and reliable instrument for measurement of the major odorous sulfur compounds has been developed. The both collection and separation is performed with the same column and simple measurement system is established. The calibration curve is linear and better response is obtained for low concentration of the sulfur gases compared to FPD method. AC power source is required but the instrument is portable and can be used for on-site analysis. The measurement is repeated automatically and the instrument is applicable to time variation analysis. The instrument proposed here is expected to use not only for environmental research but also for odor analysis and breath analysis.

References

1. Bashkova,S.; Bagreev,A.; Bandosz,T.J. Adsorption of methyl mercaptan on activated carbons. *Environmental Science Technology*, **36**, pp.2777–2782 (2002)
2. Li, X. Z., Hou, M. F., Li, F. B., Chua, H., Photocatalytic oxidation of methyl mercaptan in foul gas for odor control. *Industrial and Engineering Chemistry Research*, **45**, pp.487-494 (2006)
3. Tsai, C.H.; Lee, W.J.; Chen, C.Y.; Liao, W.T. Decomposition of CH3SH in a RF plasma reactor: reaction products and mechanisms. *Industrial and Engineering Chemistry Research*, **40**, pp.2384-2393(2001)
4. Smet, E.; Lens, P.; van Langenhove, H. Treatment of waste gases contaminated with odorous sulfur compounds. *Critical Reviews in Environmental Science and Technology*, **28(1)**, pp.89–117(1998)
5. Smet, E.; van Langenhove, H. Abatement of volatile organic sulfur compounds in odorous emissions from the bio-industry. *Biodegradation*, **9**, pp.273–284 (1998).
6. Bodenbender, J.; Wassmann, R.; Papen, H.; Rennenberg, H. Temporal and spatial variation of sulfur-gas-transfer between coastal marine sedi ments and atmosphere. *Atmospheric Environment*, **33**, pp.3487–3502 (1999).
7. Tangerman, A.; Meuwese Arends, M.T.; van Tongeren, J.H.M., A new sensitive assay for measuring volatile sulfur compounds in human breath by Tenax trapping and gas chromatography and its application in liver cirrhosis. *Clinica Chimica Acta*, **130**, pp.103–110 (1983).
8. Yaegaki, K.; Sanada, K. Biochemical and clinical factors influencing oral malodor in periodontal patients. *Journal of Periodontology*, **63**, pp.783–789 (1992).
9. Feller, L.; Blignaut, E., Halitosis: a review. *Journal of South African Dental Association*, **60**, pp.17–19 (2005).
10. Schmidt, N.F.; Missan, S.R.; Tarbet, W.J.; Cooper, A.D. The correlation between organoleptic mouth-odor ratings and levels of volatile sulfur compounds. *Oral Surgery Oral Medicine Oral Pathology*, **45**, pp.560–567 (1978).
11. Hunter, C.M.; Niles, H.P.; Lenton, P.A.; Majerus, G.J.; Vazquez,J.; Kloos, C.; Subramanyam, R.; Cummins, D. Breath-odor evaluation by detection of volatile sulfur compounds-correlation with organoleptic odor ratings. *Compendium of Continuing Education in Dentistry*, **24** *(9 suppl.)*, pp.25–28 (1995).
12. Tonzetich, J. Production and origin of oral malodor: A review of mechanisms and methods of analysis. *Journal of Periodontology*, **48**, pp.13–20 (1977).
13. Amir, E.; Shimonov, R.; Rosenberg, M. Halitosis in children. *Journal of Pediatrics*, **134**, pp.338–343 (1999).
14. Koshimune, S.; Awano, S.; Ghora, K.; Kurihara, E.; Ansai, T.; Takehara, T. Low salivary flow and volatile sulfur compounds in mouth air. *Oral Surgery Oral Medicine Oral Pathology*, **96**, pp.38–41 (2003).
15. Oho,T.; Yoshida, Y.; Shimakazi, Y.; Yamashita,Y.; Koga, T. Psychological condition of patients compla ining of halitosis. *Journal of Dentistry*, **29**, pp.31–33 (2001).
16. Awano,S.; Koshimune,S.; Kurihara,E.; Gohara,K.; Sakai, A.; Soh,I.; Hamasaki,T.; Ansai,T.; Takehara,T. The assessment of methyl mercaptan, an important clinical marker for the diagnosis of oral malodor. *Journal of Dentistry*, **32**, pp.555–559 (2004).
17. Miekisch, W.; Schubert, J.K.; Nooeldge-Schomburg G. F.E. Diagnostic potential of breath analysis-focus on volatile organic compounds. *Clinica Chimica Acta*, **347**, pp.25-29 (2004).
18. Tangerman, A.; Meuwese-Arends, M.T.; van Tongeren, J.H. Tenax trapping and gas chromatography and its application in liver disease. *Journal of Laboratory and Clinical Medicine*, **106**, pp.175–182 (1985).

19. Wardencki, W. Problems with the determination of environmental sulfur compounds by gas chromatography. *Journal of Chromatography A*, **739,** pp.1–19 (1998).
20. Cheskis, S.; Atar, E.; Amirav, Pulsed- flame photometer: A novel gas chromatography detector. *Analytical Chemistry*, **65**, pp.539–555 (1993).
21. Kelly, T.J., Kenny, D.V. Continuous determination of dimethylsulfide at part-per-trillion concentrations in air by atmospheric pressure chemical ionization mass spectrometry. *Atmospheric Environment*, **25A**, pp.2155–2160 (1991).
22. Ochiai, N., Takino, M., Daishima, S., Cardin, D.B. Analysis of volatile sulfur compounds in breath by gas chromatography-mass spectrometry using a three-stage cryogenic trapping preconcentration system. *Journal of Chromatography B*, **762**, pp.67–75 (2001).
23. Hyspler, R.; Crhova, S.; Gasparic, J.; Zadak, Z.; Cizkova, M.; Balasova, V. Determination of isoprene in human expired breath using solid-phase microextraction and gas chromatography-mass spectrometry. *Journal of Chromatography B*, **739**, pp.183–190 (2000).
24. Grote, C.; Pawliuszyn, Solid-phase microextraction for the analysis of human breath. *Analytical Chemistry*, **69**, pp.587–596 (1997).
25. Giardina, M.; Olesik, S. V. Application of low-temperature glassy carbon-coated microfibers for solid-phase microextraction analysis of simultaneous breath volatiles. *Analytical Chemistry*, **75**, pp.1604–1614 (2003).
26. Kummer, W. A.; Pitts,Jr., J. N.; Steer, R. P. Chemiluminescence reaction of ozone with olefins and sulfides. *Environmental Science and Technology*, **5**, pp.1045–1047 (1971).
27. Akimoto, H., Finlayson, B. J., Pitts, J. N. Chemiluminescent reactions of ozone with hydrogen sulfide, methyl mercaptan, dimethyl sulfide and sulfur monoxide. *Chemical Physics Letters*, **12**, pp.199–201 (1971).
28. [illegible] ozone with hydrogen sulfide and methyl mercaptan. *Journal of American Chemical Society*, **104**, pp.1196–1198 (1982).
29. Kelly, T.J., Gaffney, J. S., Phillips, M. F., Tanner, R. L. Chemiluminescent detection of reduced sulfur compounds with ozone. *Analytical Chemistry*, **55**, pp.135–138 (1983).
30. Yan, X. Sulfur and nitrogen chemiluminescence detection in gas chromatographic analysis. *Journal of Chromatography A*, [illegible]
31. Gaines, K. K.; Chatham, W. H.; Farwell, S. O. Comparison of SCD and FPD for HRGC determination of atmospheric sulfur gases. *Journal of High Resolution Chromatography*, **13**, pp.[illegible] (1990).
32. Gaffney, J.S., Spandau, D.J., Kelly, T.J., Tanner, R.L. Gas chromatographic detection of reduced sulfur compounds using ozone chemiluminescence. *Journal of Chromatography*, [illegible]
33. Burrow, P.L., Birks, J. W. Flow tube kinetics investigation of the mechanism of detection in the sulfur chemiluminescence detector. *Analytical Chemistry*, **69**, pp.1299–1306 (1997).
34. Environmental pollutants and their determination methods (in Japanese), http://www.[illegible]
35. Toda, K., Dasgupta, P. K., Li, J., Tarver, G. A., Zarus, G. M. Fluorometric field instrument for continuous measurement of atmospheric hydrogen sulfide. *Analytical Chemistry*, **73**, pp.5716–5724 (2001).
36. Ohira, S., Toda, K. Micro gas analysis system for measurement of atmospheric hydrogen sulfide and sulfur dioxide. *Lab on a Chip*, **5**, pp.1374–1379 (2005).
37. Ohira, S., Azad, M. A. K., Kuwata, [illegible], Tanaka, T., Mori, K., Toda, K. Long-term and [illegible] monitoring of atmospheric sulfur dioxide and hydrogen sulfide at Mt. Aso and Kumamoto city. *Bunseki Kagaku*, **55**, pp.109–115 (2006).

38. Azad, M. A K.; Ohira, S.; Oda, M.; Toda, K. On-site measurements of hydrogen sulfide and sulfur dioxide emissions from tidal flat sediments of Ariake Sea, Japan. *Atmospheric Environment*, **39**, pp.6077–6087 (2005).
39. Toda, K.; Ohira, S.; Tanaka, T.; Nishimura, T.; Dasgupta, P. K. Field Instrument for Simultaneous Large Dynamic Range Measurement of Atmospheric Hydrogen Sulfide, Methanethiol, and Sulfur Dioxide. *Environmental Science and Technology*, **38**, pp.1529–1536 (2004).
40. Benner, R.L., Stedman, D.H. Universal sulfur detection by chemiluminescence. *Analytical Chemistry*, **61**, pp.1268-1271(1989).
41. Inomata,Y.; Matsunaga,K.; Murai,Y.; Osada,K.; Iwasaka,Y. Simultaneous measurement of volatile sulfur compounds using ascorbic acid for oxidant removal and gas chromatography-flame photometric detection. *Journal of Chromatography A*, **864**, pp.111–119 (1999).
42. Devai, I and Delaune, R.D. Evaluation of various solid adsorbents for sampling trace levels of methanethiol. *Organic Geochemistry*, **24**, pp.941–944 (1996).
43. Clough,P.N.; Thrush, B.A. Mechanism of chemiluminescent reaction between nitric oxide and ozone. *Transactions of the Faraday Society*, **63**, pp.915-919 (1967).
44. Harrison, R.,M.; Nedwell, D.B.; Shabbeer, M.T. Factors influencing the atmospheric flux of reduced sulfur compounds fron north sea inter-tidal areas. *Atmospheric Environment*, **26A(13)**, pp.2381–2387 (1992).
45. Goldan, P.D.; Kuster, W.C.; Albritton, D.L.; Fehsenfeld, F.C. The measurement of Natural sulfur emissions from soils and vegetation: Three sites in the eastern United States revised *Journal of Atmospheric Chemistry*, **5**, pp.439–467 (1987).
46. MacTaggart, D.L.; Adams, D.F.; Farwell, S.O. Measurement of biogenic sulfur emissions from soils and vegetation using dynamic enclosure methods: Total sulfur gas emissions via MFC/FD/FPD. *Journal of Atmospheric Chemistry*, **5**, pp.417–437 (1987).

CHAPTER 5

Research Perspective and Suggestion for Future Work.

Emission of hydrogen sulfide and sulfur dioxide were studied from marine tidal flat and agricultural soil. It was observed that even the neutral sediment/soil can emit SO_2 to the atmosphere. Since the global atmospheric sulfur budget is significantly related to the global climate change, proper estimation atmospheric sulfur budget is required. Natural sources are one of the most important sources of atmospheric sulfur budget but there has a large uncertainty in the estimation of natural emission. A few works has been on SO_2 emission from natural sources. More intensive study is needed.

A new system for on-site measurement of methyl mercaptan and dimethyl sulfide has been developed. The detection was based on gas phase chemiluminescence reaction with ozone and the separation was performed depending on desorption temperature with a single adsorption/separation column without any additional separation column. The system has great potentiality for other gas measurement with a suitable adsorbent column.

APPENDIX

Appendix 1.

Principals of Diffusion Scrubber Bases Gas Measurement System

A diffusion scrubber (DS) is an excellent tool for gas analysis, and there are many types of DS devices, varying both in structure and construction. A chromatograph is a suitable tool for multi-gas analysis of the collected species. On the other hand, solid state fluorescence/absorbance detectors have been developed for the continuous measurement of target gases. The methods based on the DS collection and the subsequent detection has high sensitivities, and the detection limits can be as low as pptv levels. Accordingly, they are capable of measuring background levels, and detecting very low levels of contaminants in a clean room. DS systems have significantly contributed to our knowledge of atmospheric dynamics and atmospheric chemistry.

A denuder is defined as a gas collection devise, instead of bubbling into a solution, the gas collection is carried out on the inner wall of a tube coated with an absorbing material. Theoretical considerations on mass transfer to the walls of a cylindrical tube where the tube wall acts as a sink was first presented by Gormley and Kennedy. For a denuder of length L (m), where the wall surface is a perfect sink for the analyte gas of diffusion coefficient D (m^2 s^{-1}), being sampled at a volumetric flow rate of F (m^3 s^{-1}), the collection efficiency, f, is generally expressed as equation1 with dimensionless constants A and B *(true for situations where more than ~20% of the gas is collected)*.

$$f = 1 - A\exp(-BDL/F) \quad \text{..... (1)}$$

This equation is based on a perpendicular gas diffusion model with laminar flow during transportation along the tube. After collection, the tube is washed with a suitable liquid and the collected analyte is eluted.

Instead of the absorber being coated on the tube wall, an aqueous solution placed behind a gas permeable membrane is used as the analyte sink. We simply call this a gas diffusion scrubber (DS) here, to distinguish it from the denuder. The significant difference from the denuder is that gas can flow over the absorbing layer continuously, making it capable of continuous measurement.

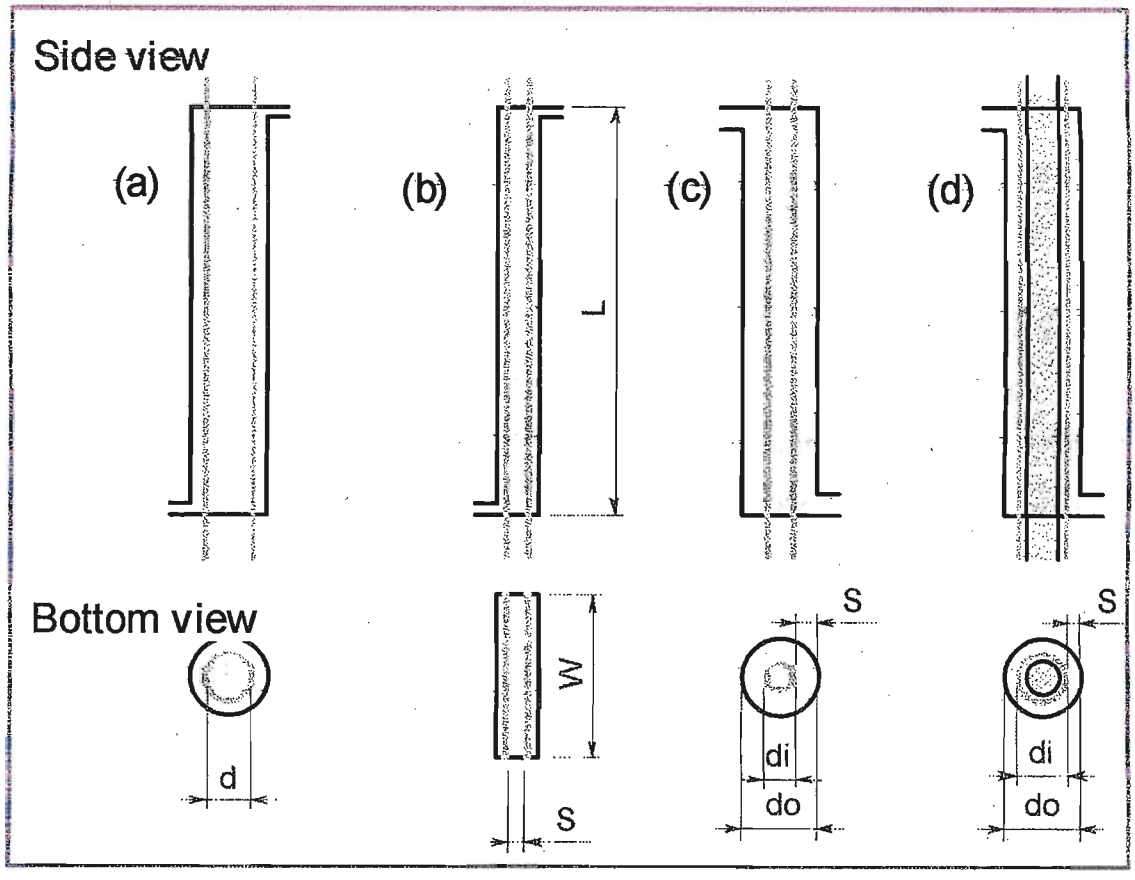

Figure A1. Schematics of gas diffusion scrubbers. (a) cylindrical DS, (b) parallel plate DS, (c) annular DS, (d) annular DS with a core.

Recently, many types of DS devices have been developed and coupled with selective reactions and novel detectors, so that the sensitivity, time resolution, portability and multi-gas measurement ability have been dramatically improved over conventional commercial instruments.

Representative DS devices and their collection efficiencies: The simplest DS structure consists of a cylindrical porous membrane tube which a sample gas flows through as Figure A1 (a). If the flow velocity and the tube diameter are small, the Reynolds number, (*Re*, equation 1) is small (< 2300) and the air stream is considered to have laminar flow.

$$Re = \frac{Ud}{\nu} = \frac{4\rho F}{\eta \pi d} \quad \text{..... (2)}$$

Here, U is flow speed, d is "the equivalent diameter" (the inner diameter of the tube in this case), ν is the kinematic viscosity of air (1.51×10^{-5} m^2 s^{-1} at 20°C 1 atm), ρ is the density of the fluid (1.205 kg/m^3 at 20°C 1 atm), and η is the viscosity of air (1.82×10^{-5} Pa s at 20°C 1

atm). If the laminar flow profile fully develops before the collection membrane is encountered, the collection efficiency, f, is expressed by Gormley and Kennedy's equation, more specifically as in equationss. 3 and 4.

$$f = 1 - 0.81905\exp(-3.6568\mu) + 0.09753\exp(-22.305\mu) + 0.0325\exp(-56.961\mu) + 0.01544\exp(-107.62\mu) \quad \text{..... (3)}$$

where

$$\mu = \pi DL/F \quad \text{..... (4)}$$

with the proviso that the wall acts as a perfect sink, and $f >\sim 0.2$ (at low collection efficiencies a different equation must be used. If the sink efficiency at the wall is very poor, μ in equation 3 must be replaced by μ^*

where

$$\mu^* = \varepsilon\mu \quad \text{..... (5)}$$

and ε is a factor related to the sink efficiency, <1. At significant collection efficiencies, terms after the 2nd one in equation 3 are small and do not contribute significantly to the total; thus the two term approximation of equation 3 is often used:

$$f = 1 - 0.819\exp(-3.657\mu) \quad \text{..... (6)}$$

There are other types of denuder, *e.g.* parallel plate (rectangular), planar or annular, and the equations for the collection efficiencies for each of these collectors have been discussed.[iii,iv] For rectangular or parallel plates with a channel width, W, and a separation between plates, S, ($S << W$) as Figure A1(b):

$$f = 1 - 0.914\exp(-7.5408\varphi) - 0.0531\exp(-83.06\varphi) - 0.01528\exp(-249.27\varphi) - 0.00681\exp(-498.15\varphi) \quad \text{for } \varphi > 0.13 \quad \text{..... (7)}$$

$$\varphi = DLW/FS \quad \text{..... (8)}$$

This equation was originally developed by Gormley. Note that the two-term approximation of equation 7 can be written as:

$$f = 1 - 0.914\exp(-3.77A_TD/FS) \quad \text{..... (9)}$$

Where, A_T is the total collection area of the parallel plate denuder.

For the annular denuder in which both the outer wall of the inner tube (d_i) and the inner wall of the outer tube (d_o) are truly effective sinks, The relevant equation will be simply obtained by substituting the applicable value of the total collector surface area and the separation between the plates, *i.e.*, since

$$A_T = \pi(d_o + d_i)L \quad \text{..... (10)}$$

and

$$S = (d_o - d_i)/2 \quad \text{..... (11)}$$

The equation for an annular denuder should be as follows[v]

$$f = 1 - 0.914 \exp(-7.54\theta DL/F) \quad (12)$$

where

$$\theta = \pi(d_o + d_i)/(d_o - d_i) \quad (13)$$

An entirely empirical equation for the collection of SO_2 with a tetrachloromercurate-coated annular denuder

$$f = 1 - 0.82\exp(-5.63\theta DL/F) \quad (14)$$

While efforts have been made to use the denuder equations for membrane based DS devices, in the case of the typical annular geometry DS, however, only the outer wall of the inner tube is effective in collecting the gas as shown in Figure A1 (c), while gas is collected on both tube walls in the annular denuder. The imperfect sink efficiency of the membrane and/or the sink chemistry causes still further complications. None of the above equations are generally applicable, holds only for specific chemistries and specific dimensions, and are not generally useful in predicting actual collection efficiencies. From equation 12 for annular denuder, equation for annular DS can be introduced by compensation of surface area. Multiply the surface area ratio of inner tube, $d_i / (d_o + d_i)$, to equation 12 and get equation 15.

$$f = 1 - 0.914\exp\left(-7.54\frac{\pi d_i}{d_o - d_i}\frac{DL}{F}\right) \quad (15)$$

This assumption simply gives the fraction, but it is effective only for the case where outer tube also acts as the sink as well as the inner tube. Therefore, this equation should give less value.

The configurations for the cylindrical and the annular DS devices are the same. In both types of scrubbers, a membrane tube is centered in a larger bore jacket tube as Figure A1 (a) and (c). The only difference is that the arrangement of liquid and gas flows is reversed. Thus, the respective DS devices may be conveniently referred to as gas-inside scrubbers (GIS) and gas-outside scrubbers (GOS) for the cylindrical DS and the annular DS.

Membrane tubes do not act as ideal sinks. The analyte gas molecules need to permeate through the membrane to reach the absorbing solution. A linear concentration gradient was formed through the membrane wall, and the performance was theoretically assessed by combination of the gradient and Gormley-Kennedy's concept.

Collected analyte quantity and concentration in the solution. The collected analyte gas in volume V_g (m^3) is the product of f, F, the collection time t (s) and the gas concentration C_g (e.g., C_g is 1×10^{-9} when the gas concentration is 1 (ppbv)

$$V_g = fFtC_g \quad (16)$$

The collected amount Q in mol is obtained from equation 16 and the equation of state with the gas temperature T (K), atmospheric pressure P (Pa) and the gas constant R (8.31 J K^{-1} mol^{-1}).

$$Q = \frac{P f F t C_g}{RT} \quad \text{..... (17)}$$

Here, f is a function of F as in equations. 3-15. Therefore, Q is almost proportional to F in the low flow rate region and constant at a high flow rate as shown in Figure A2. In these experiments, the maximum Re is *ca.* 500, and all the airflow is considered to be laminar. The supplies of gas molecules to the membrane surface and gas permeation through the membrane are the rate-determining steps in the low and high airflow ranges, respectively. The sampling rate effect depends on the membrane tube material as shown in Figure A2. In order to obtain a larger amount of analyte, the gas flow rate needs to be high enough, but note that a high F causes high water evaporation, which can affect the final concentration in the solution if the solution is pumped rather than aspirated. Generally, it is the concentration of analyte collected into the absorbing solution C_s that is measured after collection. C_s (M) can be expressed as the quotient of Q divided by the solution volume V_s (dm^3).

$$C_s = Q / V_s \quad \text{..... (18)}$$

Accordingly, it can be easily understood that the small volume DS is profitable for efficient collection.

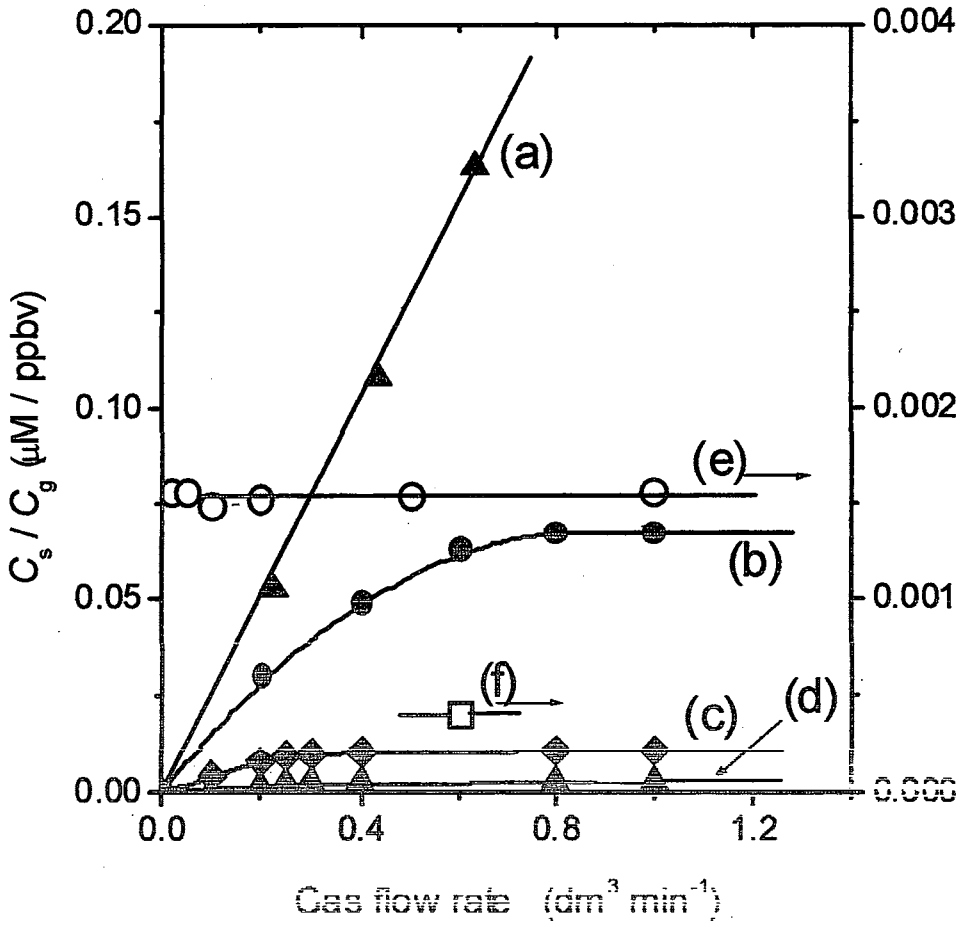

Figure A2. Effect of air sampling rate. The ordinate is the ratio of the analyte concentration collected in an absorbing solution (in μM per ppbv gas). The details of DSs, the test gas concentrations and the liquid flow rates were as follows: (a) ePTFE DS filament filled, 1.016 mm id × 60 cm, 5.5 ppbv H_2S, liquid flow rate 200 μl min^{-1}; (b) Nafion DS, 0.41 mm id × 70 cm, 11 ppbv H_2S, liquid flow 120 μl min^{-1}; (c) ePTFE DS, 2 mm id × 10 cm, 80 ppbv NO_2, 300 μl min^{-1}; (d) stopped flow 3 min, with the other conditions the same as in (c); (e) silicone DS, 0.41 mm id × 87 cm, 82 ppbv H_2S, liquid flow 100 μl min^{-1}; and (f) Teflon AF DS, 1.07 mm id × 1.5 cm, 255 ppbv H_2S, stopped flow 30 min, the ordinate scale on the right applies to (e) and (f).

Appendix 2.

Process control diagram and program set.

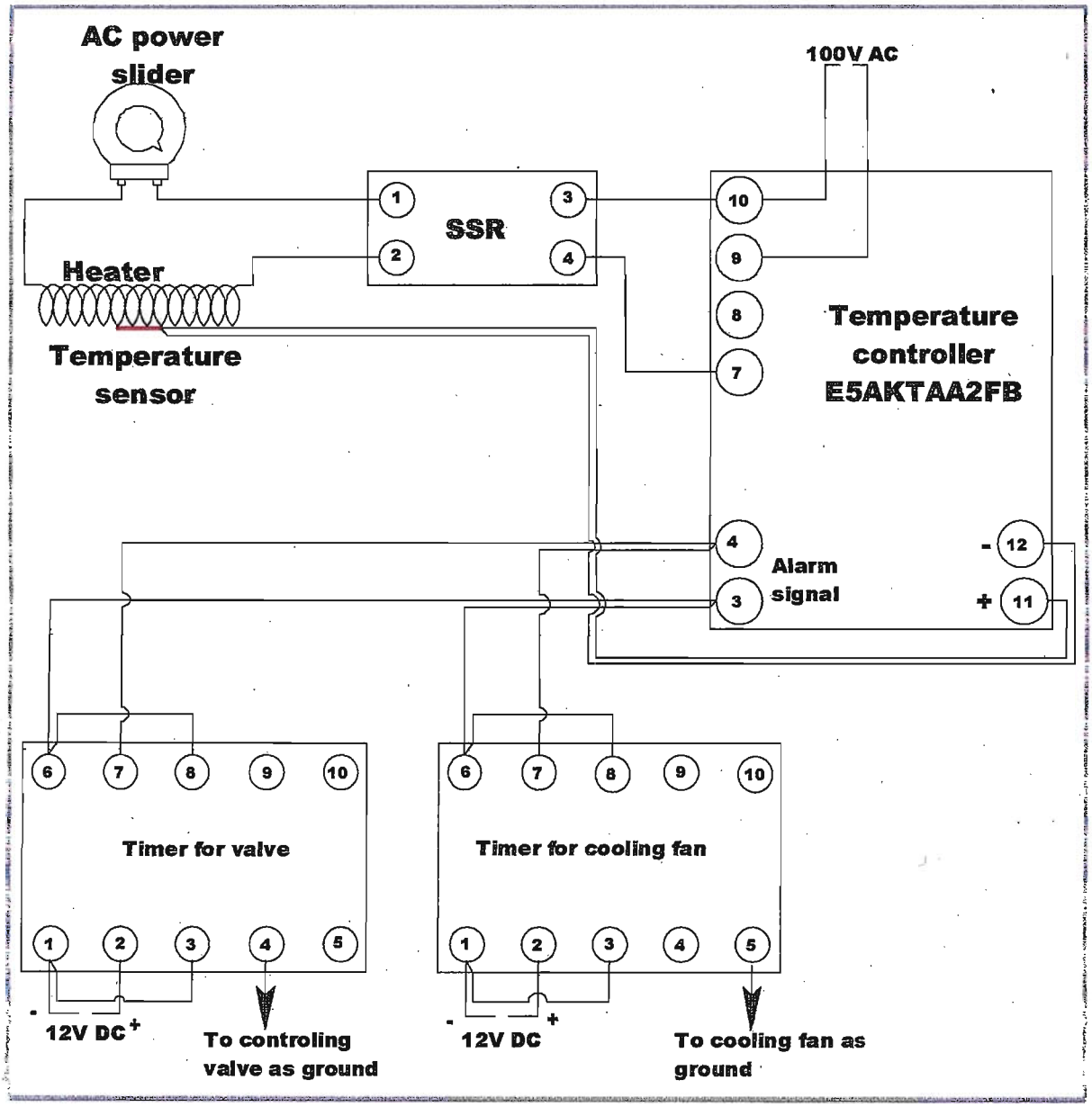

Figure A3. Instrumentation set up.

Table A1. Program set for temperature and alarm.

Program	Set Temperature	Time (min)
SP 0	-100	1
SP 1	190	1
SP 2	190	2
SP 3	280	0
SP 4	280	2
SP 5	315	0
SP 6	315	3
SP 7	0	14
Alarm 1	-400	0
Alarm 2	312	0
Alarm 3	-150	0

Table A2. Operation cycle:

Alarm signal	Restart the valve and fan controlling timer (Cycle start)				
Timer (Valve)	Valve	Time (min)	Timer (Fan)	Fan	Time (min)
Set 1 Set 2	Off On	9 5	Set 1	On	14
Set 1	Off	9	Set 2	Off	9
Alarm signal	Restart the valve and fan controlling timer				
N.B.: Valve off is measurement and cooling, valve on is sampling mode					